

## Review

## Poly beta-diketones: Prime ligands to generate supramolecular metallocusters

Guillem Aromí<sup>a</sup>, Patrick Gamez<sup>b</sup>, Jan Reedijk<sup>b,\*</sup><sup>a</sup> *Departament de Química Inorgànica, Universitat de Barcelona, Diagonal 647, 08028 Barcelona, Spain*<sup>b</sup> *Leiden Institute of Chemistry, Gorlaeus Laboratories, Leiden University, P.O. Box 9502, 2300 RA Leiden, The Netherlands*

Received 9 May 2007; accepted 22 July 2007

Available online 28 July 2007

## Contents

1. Introduction	964
2. Poly- $\beta$ -diketones	966
3. Poly- $\beta$ -diketone ligands as spacer	966
4. Metallocycles	974
5. Metallohelicates	977
6. Linear arrays	979
7. Polynuclear cage complexes	982
8. Coordination polymers	985
9. Conclusions	987
Acknowledgements	987
References	987

## Abstract

Coordination supramolecular chemistry owes its great expansion to the efforts made in designing and synthesizing new families of sophisticated multi-nucleating ligands. An emerging group of such multi-donor species is made of molecules that feature more than one beta-diketone moiety within their structure. The progressive use of such ligands in coordination chemistry is leading to a growing family of supramolecular architectures that, in many instances could have not been observed otherwise. These include homo- and heterometallic linear arrays, metallamacrocycles of different sizes, metallacoronates, triple-stranded helicates, or cage clusters of various nuclearities. This manuscript revises the advances made to date on this particular area of supramolecular coordination chemistry.

We first present a compendium of all the relevant ligands made that have been employed in this context, summarizing the synthetic routes to their preparation. Next we discuss the synthesis, structure and some aspects of the coordination compounds that have resulted from their reactions with various metals. Given the large amount and the great structural variety of the existing compounds, these have been divided into categories based on the main features of their structure. This division is in some instances discretionary, and some compounds could easily have been included in more than one category simultaneously.

© 2007 Elsevier B.V. All rights reserved.

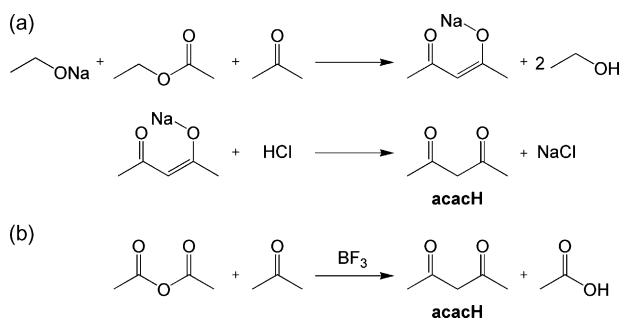
**Keywords:** Supramolecular chemistry; Multi-nucleating ligands; Multi-donor species; Beta-diketones; Heterometallic linear arrays; Metallamacrocycles; Metallacoronates; Triple-stranded helicates; Cage clusters

## 1. Introduction

The extraordinary development experienced by the topic of coordination supramolecular chemistry during the last two decades [1–3] is due to a great extent to the important effort that has been devoted to the design and preparation of novel and sophisticated multi-nucleating ligands. A very well-known

\* Corresponding author.

E-mail address: [reedijk@chem.leidenuniv.nl](mailto:reedijk@chem.leidenuniv.nl) (J. Reedijk).

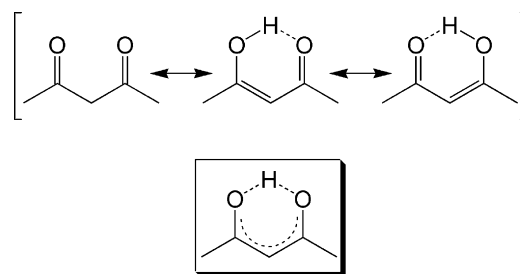


Scheme 1. Synthesis of acetylacetone (Hacac); (a) the acetone–ethyl acetate route, and (b) the acetone–acetic anhydride route.

family of such species is the group of oligo-pyridines and related *N*-heterocycles [4,5]. Many other functional groups, however, have been exploited as donors for the construction of coordination architectures by incorporation into complicated organic ligands. Among those groups are catechols [6], porphyrins [7] or calixarenes [8]. The chelating group  $\beta$ -diketone, widely used in coordination chemistry for a long time, has been increasingly encountered as a constituent of polydentate ligands in the context of metallo-supramolecular chemistry. Surprisingly, this rich subtopic of coordination chemistry had never been reviewed until very recently [9], and this conforms the subject of this account.

Acetylacetone (also known as Hacac or 2,4-pentanedione) is the simplest aliphatic  $\beta$ -diketone (Scheme 1). Its preparation was first described by Claisen more than 100 years ago [10], from the base-catalysed condensation reaction (nowadays known as the *Claisen condensation*) between acetone and ethyl acetate (Scheme 1a). Four decades later, Meerwein proposed a more efficient procedure, involving a Lewis acid, i.e.  $\text{BF}_3$  [11], as catalyst for the condensation between acetone and acetic anhydride (Scheme 1b). Since the 1940s, a number of alternative synthetic pathways have been developed employing various reactants (synthetic routes identified as the ethyl acetoacetate–ketene, methyl acetoacetate–acetic anhydride or allylene–acetic acid processes) but the acetone-process (Scheme 1b) is still the most commonly used, and the most economical as well. Throughout the years, acetylacetone has become a very important industrial chemical with many applications [12], reaching an annual production of 10,000 t in 2003.

For many decades, the  $\text{acac}^-$  ligand has been used in many fields of chemistry, and it still receives great attention from the scientific community as a result of its valuable intrinsic chemical and physical properties. Metal acetylacetonates are very stable, commercially available coordination compounds, very often used as catalyst precursors [13,14]. In that context,  $[\text{M}^{n+}(\text{acac})_n]$  complexes have found many applications in organometallic chemistry where they are commonly employed as reactants to generate complex (heteronuclear) organometallic compounds [15,16]. Owing to their excellent volatility, metal acetylacetonates are often used for the chemical vapour deposition of metal and metal oxide thin films [17], a topical field of research in material science [18]. A series of  $\text{acac}^-$  complexes have also proven to be valuable chemical tools to establish the



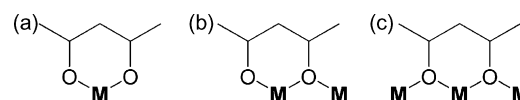
Scheme 2. Tautomerism of Hacac.

radius of ions, through the determination of the corresponding M–O bond lengths by X-ray crystallography [19].

The widespread use of acetylacetonate as chelating ligand in coordination chemistry and the stability of its complexes with a number of metal ions [20] originate from its chemical properties, determined by the keto–enol tautomerism illustrated in Scheme 2. At ambient conditions, it is generally accepted that Hacac mainly exists in its enolic form in the gas and liquid phases [21]. The  $\text{pK}_a$  of Hacac in water amounts to 8.9 [22]; Thus, Hacac can be easily deprotonated, and the resulting  $\text{acac}^-$  moiety can act as an anionic bidentate ligand, which can bind to metal ions in different coordination modes (Scheme 3). Usually, metals react with Hacac (or its salt) to form bonds with the two oxygen atoms (Scheme 3a). A typical example of this chemistry is  $\text{Mn}(\text{acac})_3$  [23], which represents one of the most prepared compounds in inorganic chemistry laboratory classes [24]. The  $\mu$  (Scheme 3b) [25] and  $\mu_3$  (Scheme 3c) [26] coordination modes have also been observed. Finally, the weak  $\pi$ -acidic character of  $\text{acac}^-$  is comparable to that of ammonia, in contrast to bipyridine, which is characterized by its important  $\pi$ -acceptor ability. Owing to the simplicity of the preparation of  $\beta$ -diketones, many Hacac analogues are known. For instance, 1,3-diphenylpropane-1,3-dione (Hdba) has also been used extensively in coordination chemistry (334 hits in the Cambridge Structural Database; version 5.28, November 2006).

In the present paper, the attention is directed towards metallo-supramolecular networks whose assemblies involve ligands containing various  $\beta$ -diketone units. The  $\text{acac}^-$  ligand alone has been extensively used in the formation of metal-organic frameworks, either as precursors for the synthesis of metal coordination clusters [27,28] with interesting magnetic properties [29], or as coordination synthons for the creation of extended supramolecular architectures [30,31]. In the latter case, since  $[\text{M}^{\text{II}}(\text{acac})_2]$  complexes are usually square-planar [32], they can be used as  $180^\circ$  building blocks with ‘blocked’ equatorial sites and axial positions available for coordination.

The versatility of  $\beta$ -diketone ligands associated to their straightforward synthesis have prompted the imagination and creativity of research scientists who have built-up  $\text{acac}^-$ -type



Scheme 3. Coordination modes observed for the  $\text{acac}^-$  ligand. (a) Acetylacetonato; (b)  $\mu$ -acetylacetonato; (c)  $\mu_3$ -acetylacetonato.

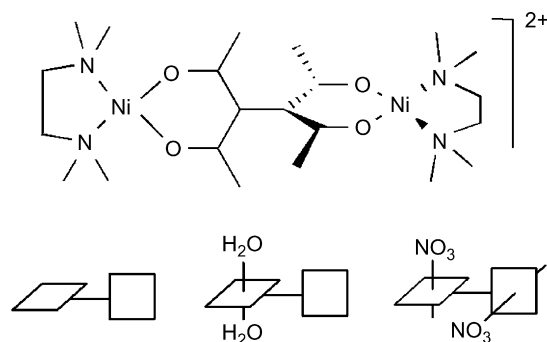
moieties into ligands specifically designed for the preparation of beautiful metallo-supramolecules [33,34]. The association of two or more  $\beta$ -diketone moieties within single-molecules has also been achieved [35,36], its application as ligands having thus favored the formation of polynuclear complexes [37].

The scope of the present review encompasses the utilization of poly- $\beta$ -diketones to create metallo-supramolecular assemblies with applications in crystal engineering or magnetochemistry.

## 2. Poly- $\beta$ -diketones

In the present section the structure and synthesis of the poly- $\beta$ -diketones used during the past 50 years for the preparation of metallosupramolecular aggregates are reviewed. A non-exhaustive list is compiled in Table 1, together with their chemical structure, these of the reactants used for their preparation and the references where the syntheses are reported. As evidenced in this table, intricate polydentate ligands can be prepared in a straightforward manner, very often via a one-step reaction involving commercially, readily available reactants. From the 54 ligands presented in this table, 27, i.e. H<sub>2</sub>L2, H<sub>2</sub>L3, H<sub>2</sub>L4, H<sub>3</sub>L5, H<sub>4</sub>L6, H<sub>2</sub>L14, H<sub>2</sub>L15, H<sub>3</sub>L16, H<sub>4</sub>L17, H<sub>2</sub>L18, H<sub>2</sub>L21, H<sub>2</sub>L22, H<sub>2</sub>L24, H<sub>2</sub>L26, H<sub>2</sub>L32, H<sub>2</sub>L33, H<sub>2</sub>L34, H<sub>2</sub>L35, H<sub>2</sub>L36, H<sub>2</sub>L37, H<sub>2</sub>L42, H<sub>2</sub>L43, H<sub>2</sub>L44, H<sub>2</sub>L45, H<sub>2</sub>L46, H<sub>2</sub>L47, H<sub>2</sub>L51, have been synthesized applying the procedure described by Claisen in 1889, which is the condensation between a ketone and an ester (Scheme 1a) [10]. However, the efficiency of the Claisen condensation has been improved through the use of more effective and stronger bases, such as sodium hydride or sodium amide, and solvents like 1,2-dimethoxyethane (DME). A second synthetic pathway to poly- $\beta$ -diketones consists in the alkylation of a  $\beta$ -diketone with a dihalogeno derivative, under basic conditions (Table 1, H<sub>2</sub>L8–H<sub>2</sub>L10). A possible simple route to modified poly- $\beta$ -diketone derivatives is based on the condensation of an amine with one of the carbonyl functions of a 1,3,5-triketone (H<sub>2</sub>L29). Finally, a number of outstanding poly- $\beta$ -diketones have been produced using different unusual methods. The bis-Hacac compound H<sub>2</sub>L1 is obtained by cerium(III)-catalysed oxidative coupling of two Hacac molecules. The triketone H<sub>2</sub>L38 is prepared from dehydroacetic acid, by decarboxylative ring-opening under extreme conditions. H<sub>2</sub>L48 and H<sub>2</sub>L49 are synthesized by reaction of the corresponding dialkylmalonate with oxalyl chloride. H<sub>2</sub>L27 and H<sub>2</sub>L28 are produced by ring-opening of a dioxione in the appropriate solvent, in the presence of phenyl isothiocyanate. The bis-Hacac derivative H<sub>2</sub>L54 is generated by acidic hydrolysis of the corresponding enamine. The chiral fluorinated ligand H<sub>2</sub>L7 has been prepared by reaction of the Grignard reagent obtained from D-3-bromocamphor with diethyl hexafluoroglutarate.

Table 2 summarizes the metals with which, the ligands described have formed structurally characterized complexes so far. Most of the X-ray structures mentioned in this compilation will be presented in the following sections.



Scheme 4. Representation of the core structure of complexes **1**, **2** and **3** (top) and position of axial ligands (bottom).

## 3. Poly- $\beta$ -diketone ligands as spacer

Some complexes containing a poly- $\beta$ -diketone have this ligand acting only as spacer between two or more metals, each chelated by one 1,3-diketonate, with no additional bridges between them. The most recurrent ligand in this category of compounds is the dianion of 1,1,2,2-tetraacetyethane (H<sub>2</sub>L1, Table 1). Thus, L1<sup>2-</sup> has served as bridge within dinuclear complexes of Cu<sup>II</sup>, Ni<sup>II</sup>, Co<sup>II</sup>, Co<sup>III</sup>, Ru<sup>II</sup> and Ru<sup>III</sup>. These compounds were prepared to study the interaction between two metals within a well-defined molecular framework as manifested through the electrochemical, magnetic, or spectroscopic properties. One of the earliest papers [38] reports a series of compounds featuring the basic structure shown in Scheme 4(top) with different numbers and types of axial ligands (Scheme 4, bottom) and with formulae [Ni<sub>2</sub>(L1)(tmen)<sub>2</sub>](BPh<sub>4</sub>)<sub>2</sub> (**1**), [Ni<sub>2</sub>(L1)(tmen)<sub>2</sub>(H<sub>2</sub>O)<sub>2</sub>](ClO<sub>4</sub>)<sub>2</sub> (**2**) and [Ni<sub>2</sub>(L1)(tmen)<sub>2</sub>(NO<sub>3</sub>)<sub>2</sub>] (**3**), where tmen = tetramethylethylenediamine. The molecular structure of complexes **1**, **2** and **3** was deduced by combining a variety of techniques, including magnetic measurements and UV spectroscopy. Thus, compound **1** was found to be diamagnetic (as expected for two square-planar Ni<sup>II</sup> ions), complex **2** exhibited the magnetic moment expected for the presence of one octahedral Ni<sup>II</sup> center per molecule, whereas **3** had a magnetic response at room temperature corresponding to two *S* = 1 centers per molecule (two octahedral *d*<sup>8</sup> ions, as a result of NO<sub>3</sub><sup>-</sup> ligands bridging Ni<sup>II</sup> centers axially). A few years later, a Cu<sup>II</sup> analogue of these complexes, [Cu<sub>2</sub>(L1)(tmen)<sub>2</sub>(H<sub>2</sub>O)<sub>2</sub>](ClO<sub>4</sub>)<sub>2</sub> (**4**) was reported and the spectroscopic and electrochemical properties were studied as a function of the solvent and its donor character [39]. The first single-crystal X-ray structure obtained for this series of compounds [12] corresponded to [Cu<sub>2</sub>(L1)(tmen)<sub>2</sub>](ClO<sub>4</sub>)<sub>2</sub> (**5**, Fig. 1), which, together with [Cu<sub>2</sub>(L1)(tmen)<sub>2</sub>](BPh<sub>4</sub>)<sub>2</sub> (**6**), was studied through variable temperature magnetic measurements, as well as by EPR and UV–vis absorption spectroscopy. These studies revealed that the L1<sup>2-</sup> ligand mediates a moderate antiferromagnetic interaction between the Cu<sup>II</sup> centers. By contrast, a similar compound involving the terminal chelating ligand bipyridylamine (bpya), [Cu<sub>2</sub>(L1)(bpya)<sub>2</sub>(O<sub>2</sub>CCF<sub>3</sub>)<sub>2</sub>] (**7**), was found to exhibit two almost uncoupled Cu<sup>II</sup> ions within the molecule, whereas the Co<sup>II</sup> quasi-analogue [Co<sub>2</sub>(L1)(bpya)<sub>4</sub>](O<sub>2</sub>CCH<sub>3</sub>)<sub>2</sub> (**8**, Fig. 2)

Table 1  
Poly- $\beta$ -diketones and experimental procedures for their preparation

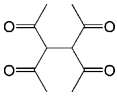
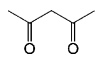
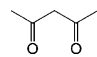
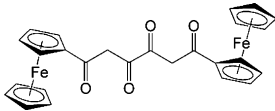
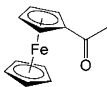
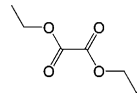
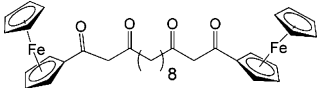
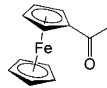
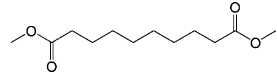
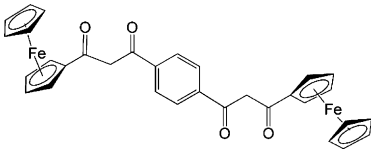
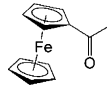
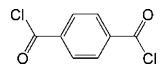
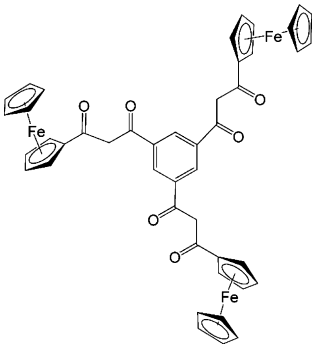
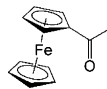
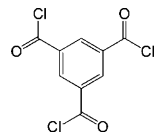
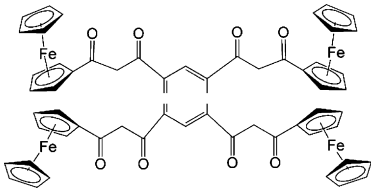
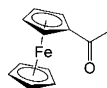
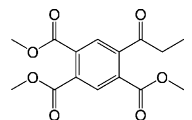
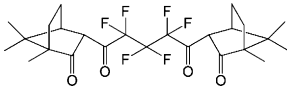
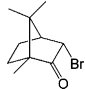
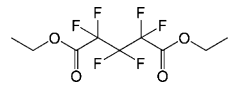
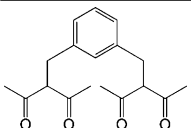
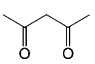
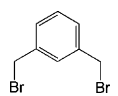
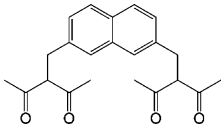
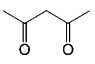
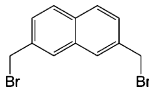
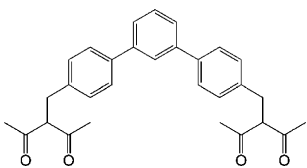
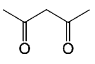
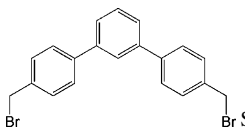
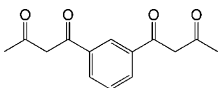
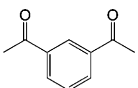
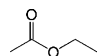
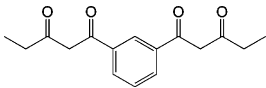
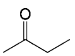
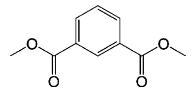
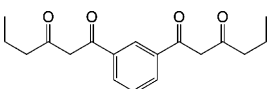
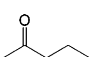
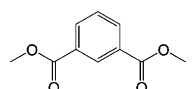
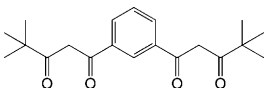
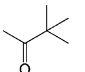
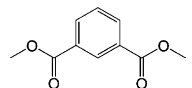
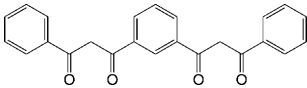
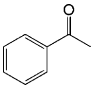
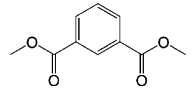
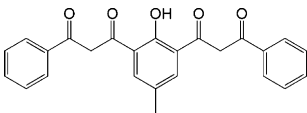
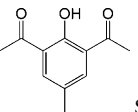
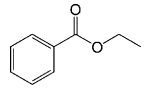
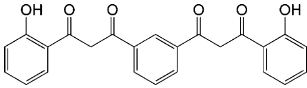
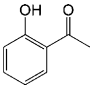
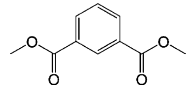
Ligand	Abbrev.	Reactants <sup>a</sup> used for the preparation of the ligands		References	
	H <sub>2</sub> L1			Ce(NO <sub>3</sub> ) <sub>3</sub> ·3H <sub>2</sub> O MeOH	[106]
	H <sub>2</sub> L2			KH/THF	[107]
	H <sub>2</sub> L3			KH/THF	[107]
	H <sub>2</sub> L4			KH/THF	[107]
	H <sub>2</sub> L5			KH/THF	[107]
	H <sub>2</sub> L6			KH/THF	[107]
	H <sub>2</sub> L7			Mg/Et <sub>2</sub> O	[46]

Table 1 (Continued)

Ligand	Abbrev.	Reactants <sup>a</sup> used for the preparation of the ligands		References
	H <sub>2</sub> L8			K/ <i>tert</i> -BuOH, KI [108]
	H <sub>2</sub> L9		 See Ref. [109]	K/ <i>tert</i> -BuOH, KI [35,108]
	H <sub>2</sub> L10		 See Ref. [51]	<i>tert</i> -BuOK/ <i>tert</i> -BuOH [51]
	H <sub>2</sub> L11			Na [110]
	H <sub>2</sub> L12			NaNH <sub>2</sub> /Et <sub>2</sub> O [104]
	H <sub>2</sub> L13			NaNH <sub>2</sub> /Et <sub>2</sub> O [104]
	H <sub>2</sub> L14			NaNH <sub>2</sub> /Et <sub>2</sub> O [52]
	H <sub>2</sub> L15			NaH/DME [69,111]
	H <sub>3</sub> L16	 See Ref. [112]		NaH/DME [112]
	H <sub>4</sub> L17			NaH/DME [53]

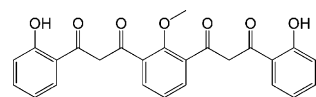

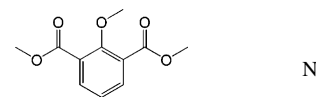
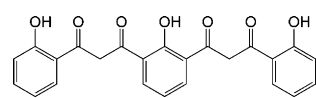

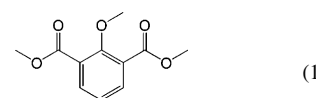
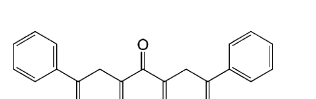
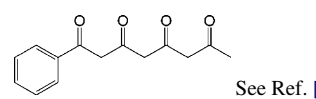
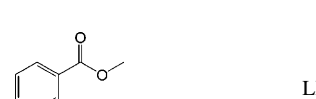
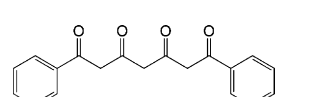
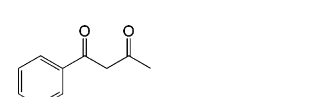
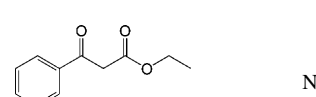
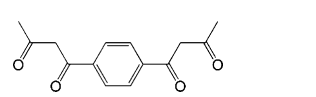

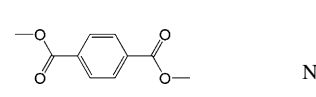
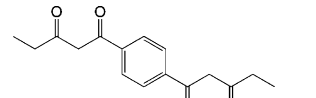

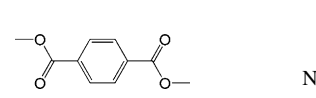
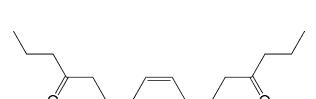

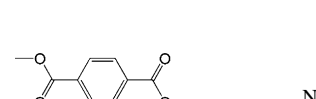
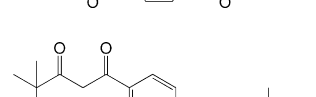

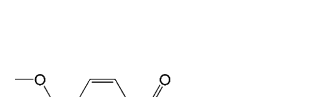
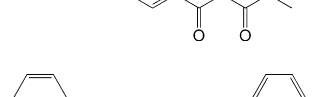

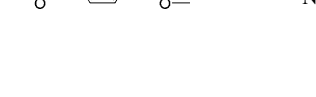
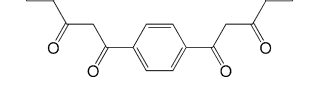

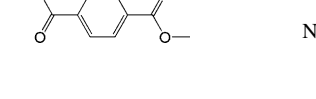
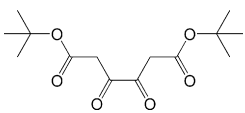
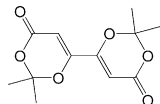
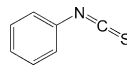
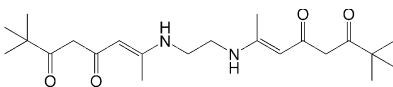
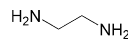
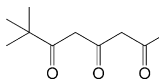
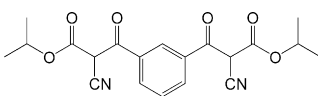
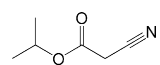
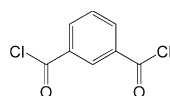
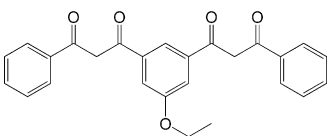
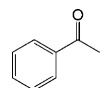
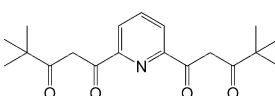
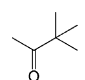
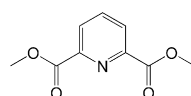
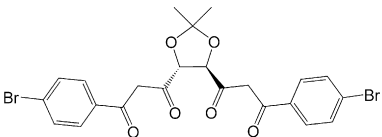
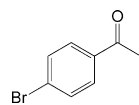
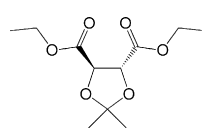
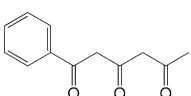
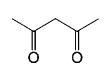
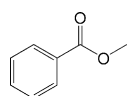
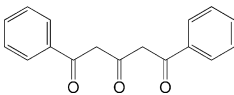
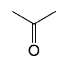
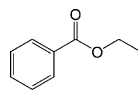
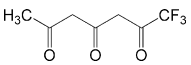
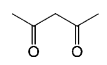
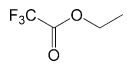
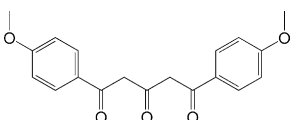
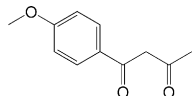
	H <sub>4</sub> L18			NaH/DME	[93]
	H <sub>5</sub> L19			(1) NaH/DME; (2) BBr <sub>3</sub> /CH <sub>2</sub> Cl <sub>2</sub>	[93]
	H <sub>2</sub> L20	 See Ref. [113]		LDA/THF	[113,114]
	H <sub>2</sub> L21			NaH/THF, LDA/THF	[115]
	H <sub>2</sub> L22			NaNH <sub>2</sub> /Et <sub>2</sub> O	[62]
	H <sub>2</sub> L23			NaNH <sub>2</sub> /Et <sub>2</sub> O	[104]
	H <sub>2</sub> L24			NaNH <sub>2</sub> /Et <sub>2</sub> O	[62]
	H <sub>2</sub> L25			NaNH <sub>2</sub> /Et <sub>2</sub> O	[104]
	H <sub>2</sub> L26			NaNH <sub>2</sub> /Et <sub>2</sub> O	[111]
	H <sub>2</sub> L27	 See Ref. [116]		EtOH	[64]

Table 1 (Continued)

Ligand	Abbrev.	Reactants <sup>a</sup> used for the preparation of the ligands		References
	H <sub>2</sub> L28	 See Ref. [116]	 <i>tert</i> -BuOH	[63]
	H <sub>2</sub> L29	  See Ref. [117]	MeOH	[67,76]
	H <sub>2</sub> L30	 	Et <sub>3</sub> N/MgCl <sub>2</sub> , CH <sub>3</sub> CN	[71]
	H <sub>2</sub> L31	 See Ref. [72]	NaH/THF	[72]
	H <sub>2</sub> L32	 	NaOMe/THF	[91]
	H <sub>2</sub> L33	 	NaNH <sub>2</sub> /Et <sub>2</sub> O	[74]
	H <sub>2</sub> L34	 	NaH/DME	[118]
	H <sub>2</sub> L35	 	NaH/DME	[119]
	H <sub>2</sub> L36	 	NaH/DME	[83,114]
	H <sub>2</sub> L37	 See Ref. [120]	NaH/DME	[78,114]

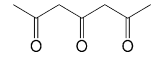
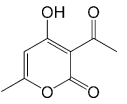
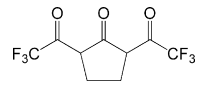
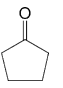
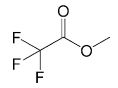
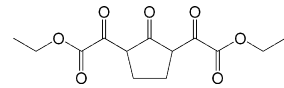
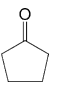
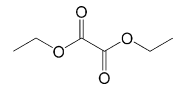
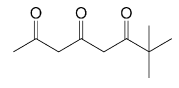
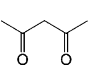
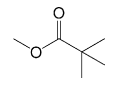
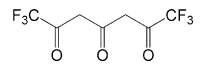
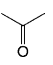
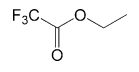
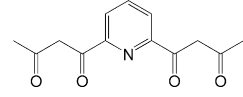
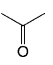
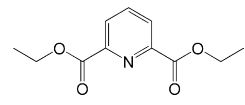
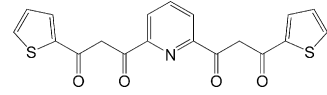
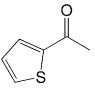
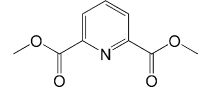
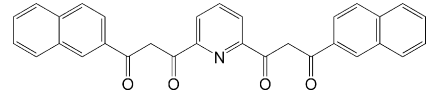
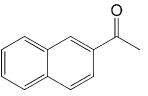
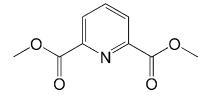
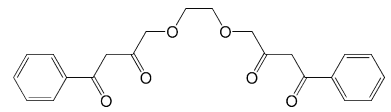
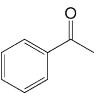
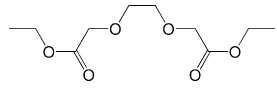
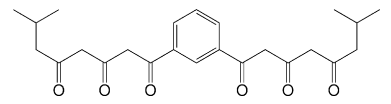
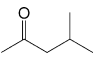
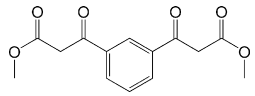
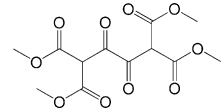
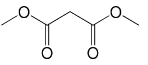
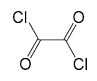
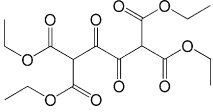
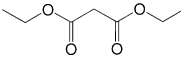
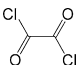
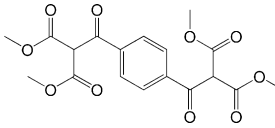
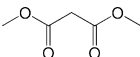
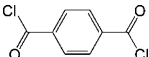
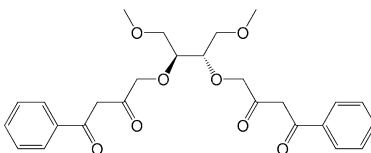
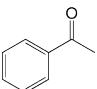
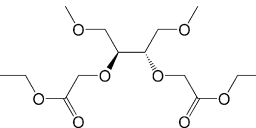
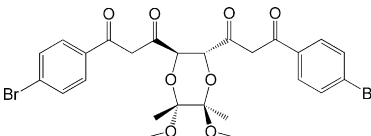
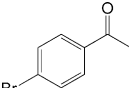
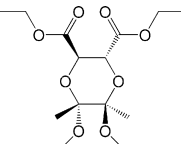
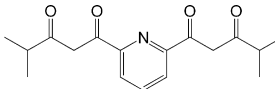
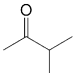
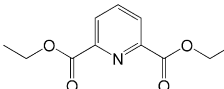
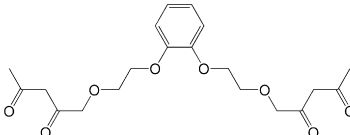
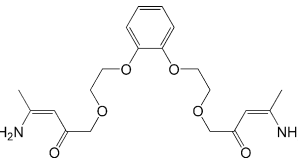
	H <sub>2</sub> L38		HCl	Reflux NaOH/Ba(OH) <sub>2</sub>	[121]
	H <sub>2</sub> L39			LiH/DME	[122]
	H <sub>2</sub> L40			NaOEt/Et <sub>2</sub> O	[123]
	H <sub>2</sub> L41			NaH/THF	[117]
	H <sub>2</sub> L42			NaH/DME	[124]
	H <sub>2</sub> L43			Na/EtOHToluene	[86]
	H <sub>2</sub> L44			NaOMe/THF	[91]
	H <sub>2</sub> L45			NaOMe/THF	[91]
	H <sub>2</sub> L46		 See Ref. [125]	NaNH <sub>2</sub> /Et <sub>2</sub> O	[90,126]
	H <sub>4</sub> L47		 See Ref. [127]	NaH/THF	[94]
	H <sub>2</sub> L48			MeLi/THF, MgCl <sub>2</sub> , R <sub>4</sub> NCI/H <sub>2</sub> O	[128]



Table 1 (Continued)

Ligand	Abbrev.	Reactants <sup>a</sup> used for the preparation of the ligands		References
	H <sub>2</sub> L49			MeLi/THF, MgCl <sub>2</sub> , R <sub>4</sub> NCl/H <sub>2</sub> O [128]
	H <sub>2</sub> L50			MeLi/THF, MgCl <sub>2</sub> , R <sub>4</sub> NCl/H <sub>2</sub> O [98]
	H <sub>2</sub> L51		 See Ref. [99]	NaNH <sub>2</sub> /THF [99]
	H <sub>2</sub> L52		 See Ref. [129]	NaNH <sub>2</sub> /Et <sub>2</sub> O [100]
	H <sub>2</sub> L53			Na/EtOH, Et <sub>2</sub> O [86,101]
	H <sub>2</sub> L54	 See Ref. [130]	HCl (H <sub>2</sub> O)	EtOH [130]

<sup>a</sup> The reactants are commercially available unless otherwise stated.

Table 2

Metal ions coordinated by the ligands presented in Table 1

Ligand	Metals + references
H <sub>2</sub> L1	Ni [38], Cu [12,39–42], Co [36,40], Ru [43]
H <sub>2</sub> L2	Pd [44], Ir [44]
H <sub>2</sub> L3	Pd [44]
H <sub>2</sub> L4	Pd [44], Ru [44]
H <sub>3</sub> L5	Pd [44]
H <sub>4</sub> L6	Pd [44]
H <sub>2</sub> L7	Rh [45,46]
H <sub>2</sub> L8	Cu [47]
H <sub>2</sub> L9	Cu [35,48,49], V [50]
H <sub>2</sub> L10	Cu [51]
H <sub>2</sub> L11	Cu [52]
H <sub>2</sub> L12	Cu [52], Fe [52]
H <sub>2</sub> L13	Cu [52]
H <sub>2</sub> L14	Cu [52,103], Fe [52]
H <sub>2</sub> L15	Ti [69], V [69], Mn [69], Fe [69], Eu [72], Nd [72], Sm [72], Y [72], Gd [72]
H <sub>3</sub> L16	Cu [54,55,105], Mn [58,59,92], Ni [59], Co [57]
H <sub>4</sub> L17	Cu [53], Ni [53], Mn [53], Co [53], Fe [95]
H <sub>4</sub> L18	Mn [102], Fe [102]
H <sub>5</sub> L19	Mn [56,93], Ni [56], Co [56]
H <sub>2</sub> L20	Co [60]
H <sub>2</sub> L21	Co [60], (U, Cu) [84,85], (U, Zn) [84,85], (U, Ni) [84,85], (U, Co) [84,85], (U, Mn) [84,85], (U, Fe) [84,85]
H <sub>2</sub> L22	Cu [62], Fe [62], Ga [62]
H <sub>2</sub> L23	Cu [62,104], Fe [62]
H <sub>2</sub> L24	Cu [62,104], Fe [62,98], Ga [98]
H <sub>2</sub> L25	Cu [104], Fe [62]
H <sub>2</sub> L26	Ni [61], Co [61], Fe [62], Zn [61]
H <sub>2</sub> L27	(Cu, Ca) [64], (Cu, Na) [64,65], Ca [65], Mn [65], Cd [65]
H <sub>2</sub> L28	Cu [63], (Cu, Na) [64], (Cu, K) [64], Ca [65], Mn [65], Cd [65]
H <sub>2</sub> L29	Cr [67]
H <sub>2</sub> L30	Fe [71]
H <sub>2</sub> L31	Eu [72], Nd [72]
H <sub>2</sub> L32	Fe [73], (Fe, K) [71], (Fe, Sr) [73], (Fe, Ba) [91], (Fe, La) [91], Co [91]
H <sub>2</sub> L33	Fe [74], Ga [74], (Li, Ga) [74], Ni [75]
H <sub>2</sub> L34	Cu [76]
H <sub>2</sub> L35	Ni [82], Co [81]
H <sub>2</sub> L36	Cu [83], Ni [83]
H <sub>2</sub> L37	Cu [78]
H <sub>2</sub> L38	Cu [79]
H <sub>2</sub> L39	Cu [76]
H <sub>2</sub> L40	Ni [80]
H <sub>2</sub> L41	
H <sub>2</sub> L42	Cu [85]
H <sub>2</sub> L43	(Cu, Ba) [86,87], (Ni, Ba) [86,87], (Cu, Pb) [87], (Ni, Pb) [87], (Co, Pb) [87], (Co, Ba) [87], (Cu, Ln; Ln = La, Ce, Pr, Nd, Sm, Eu, Gd, Tb, Dy, Ho, Er, Tm, Yb, Lu, Y) [88]
H <sub>2</sub> L44	(Fe, K) [91]
H <sub>2</sub> L45	(Fe, K) [91]
H <sub>2</sub> L46	(Cu, M; M = K, Rb, Cs) [90]
H <sub>4</sub> L47	Cu [94]
H <sub>2</sub> L48	Fe [96], Mn [97], Co [97], Ni [97]
H <sub>2</sub> L49	Fe [96]
H <sub>2</sub> L50	Fe [98]
H <sub>2</sub> L51	Cu [99]
H <sub>2</sub> L52	Ga [100]
H <sub>2</sub> L53	Mn [101]
H <sub>2</sub> L54	(Ni, Cs) [90]

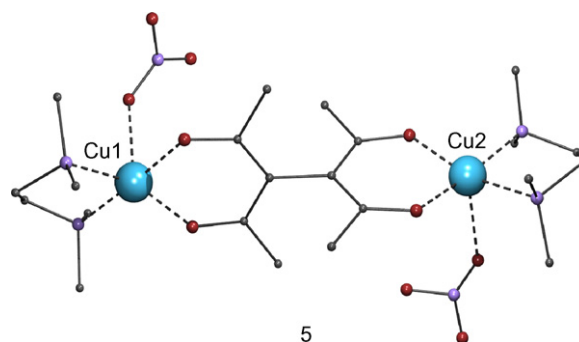


Fig. 1. PovRay representation of complex  $[\text{Cu}_2(\text{L1})(\text{tmen})_2](\text{ClO}_4)_2$  (**5**) [12]. Code for atoms: large, metal; dark (or red) medium size, oxygen; light (or purple) medium size, nitrogen; small, carbon. Hydrogen atoms not shown. (For interpretation of the references to color in this figure legend, the reader is referred to the web version of the article.)

clearly showed the presence of ferromagnetic exchange [40]. The latter was corroborated by Extended Hückel Molecular Orbital Calculations, which revealed the presence of two almost degenerate single occupied molecular orbitals (SOMOs). The X-ray structure of the bipyridine (bpy) and phenantroline (phen)  $\text{Cu}^{\text{II}}$  derivatives,  $[\text{Cu}_2(\text{L1})(\text{bpy})_2(\text{ClO}_4)_2(\text{H}_2\text{O})_2]$  (**9**) [41] and  $[\text{Cu}_2(\text{L1})(\text{phen})_2\text{Cl}_2](\text{ClO}_4)_2$  (**10**) [42] have been reported; they all have been found to display very weak antiferromagnetic interactions within the molecule. Much more recently [43], a group of electroactive Ru(III) or Ru(II) dinuclear complexes were prepared with formulae  $[\text{Ru}_2(\text{L1})(\text{ch})_4]$  (Hch is a 1,3-diketone chelate; 2,4-pentadione (**11**), or 2,2,6,6-tetramethyl-3,5-heptanedione (**12**)) and  $[\text{Ru}_2(\text{L1})(\text{bpy})_4](\text{PF}_6)_2$  (**13**), together with their corresponding mononuclear analogues  $[\text{Ru}(\text{ch})_2(\text{acac})]$  and  $[\text{Ru}_2(\text{bpy})_2(\text{acac})](\text{PF}_6)_2$ . All dinuclear compounds could be separated into the meso ( $\Delta-\Delta$ ) isomer and the racemic ( $\Delta-\Lambda$ ) and ( $\Lambda-\Lambda$ ) mixture, and were studied by  $^1\text{H}$  NMR. This series of compounds was prepared with the aim of investigating the capacity of the ligand  $\text{L1}^{2-}$  to couple both metals electronically. This was done by studying the comproportionation constants,  $K_c$  for the mixed-valence states ( $\text{Ru}^{\text{II}}-\text{Ru}^{\text{III}}$ ) and ( $\text{Ru}^{\text{III}}-\text{Ru}^{\text{IV}}$ ) as followed by electrochemical measurements and controlled by electronic spectra. It was found that the  $K_c$  values are higher than expected, indicating a low degree of electronic communication as mediated by the  $\text{L1}^{2-}$  ligand, which was ascribed to the fact that both chelate

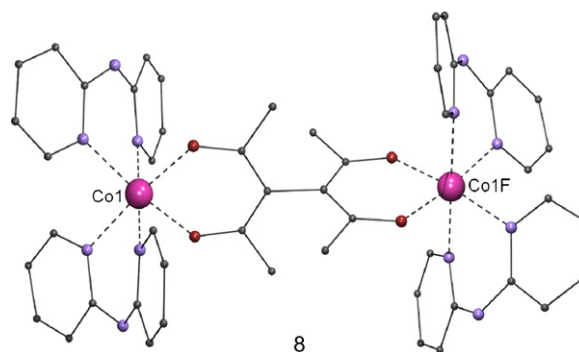
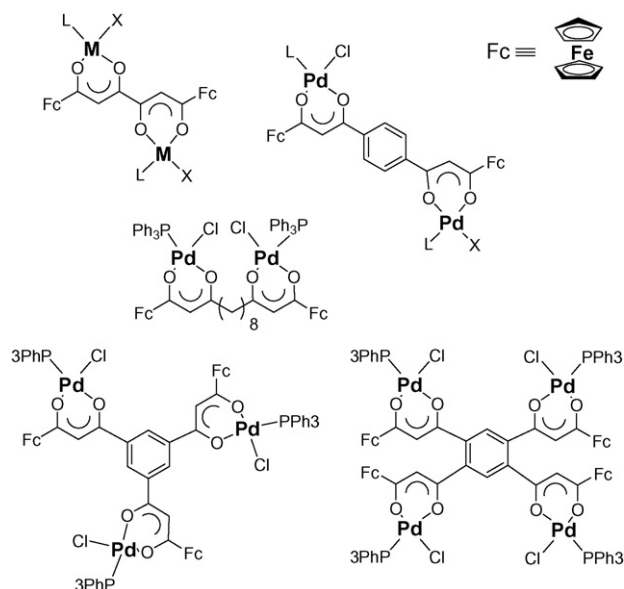


Fig. 2. PovRay representation of complex  $[\text{Co}_2(\text{L1})(\text{bpya})_4](\text{O}_2\text{CCH}_3)_2$  (**8**) [40]. Code for atoms as in Fig. 1. Hydrogen atoms not shown.



Scheme 5. Representation of the structure of complexes **14–22**, made with ligands  $H_2L_2$ ,  $H_2L_3$ ,  $H_2L_4$ ,  $H_3L_5$  and  $H_4L_6$ .

rings of the bridging ligands are nearly perpendicular to each other.

A different family of complexes falling under this category is made from ferrocenyl substituted bis-, tris- or tetrakis-1,3-diketone ligands  $H_2L_2$ ,  $H_2L_3$ ,  $H_2L_4$ ,  $H_3L_5$  and  $H_4L_6$  (Table 1) [44]. Thus, the series of compounds  $[Pd_2(L_2)(PPh_3)_2Cl_2]$  (**14**),  $[Pd_2(L_2)(PTol_3)_2Cl_2]$  (**15**),  $[Ir_2(L_2)(C_5Me_5)_2Cl_2]$  (**16**),  $[Pd_2(L_2)(C_3H_5)_2]$  (**17**),  $[Pd_2(L_3)(PPh_3)_2Cl_2]$  (**18**),  $[Pd_2(L_4)(PPh_3)_2Cl_2]$  (**19**),  $[Ru_2(L_4)(p-Cymol)_2Cl_2]$  (**20**),  $[Pd_3(L_5)(PPh_3)_3Cl_3]$  (**21**) and  $[Pd_4(L_6)(PPh_3)_4Cl_4]$  (**22**) were prepared and characterized (Scheme 5). The single-crystal structure of **15** was determined.

Finally, two interesting compounds in this category are these formed with the homochiral ligands 3,3'-hexafluoroglutarylbis-(1*R*)-camphorate (or the corresponding (1*S*,1*S*) enantiomer;  $H_2L_7$ ) with carbonyl and  $Rh^I$  [45,46]. The chiral bis- $\beta$ -diketone binds two rhodium atoms and folds itself in a helical manner to allow intramolecular metal–metal interactions. The helicity of the ligand introduces another element of chirality depending on the sense of the screw; *M* or *P*. The complementarity of both diastereoisomers of  $[Rh_2(L_7)(CO)_4]$  (**23**), (1*R*)-*M*-(1*R*) and (1*R*)-*S*-(1*R*), causes these to crystallize together in the form of alternate infinite chains (Fig. 3).

#### 4. Metallocycles

A large portion of polynuclear complexes featuring poly- $\beta$ -diketonate ligands constitute metallocycles. These are molecular macrocycles containing two or more metals, which are linked within this cycle through an equal number of atom strings (mostly made of C and O) from the ligand framework. The majority of metallocycles reviewed here fall in the specific category of metallacyclophanes. These are metallocycles that feature aromatic rings as integral part of the cyclic moiety.

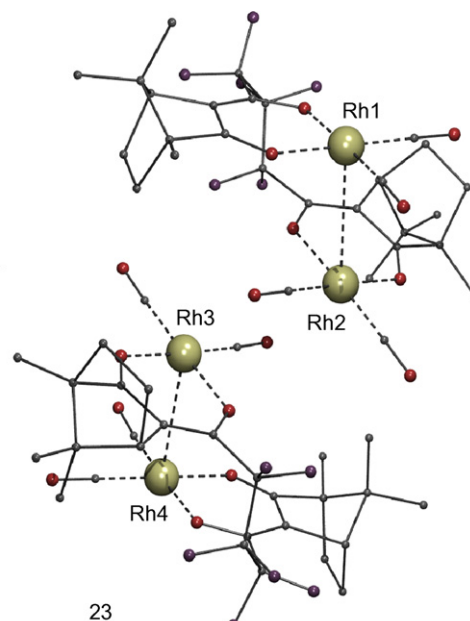


Fig. 3. PovRay representation of co-crystallized stereoisomers of  $[Rh_2(L_7)(CO)_4]$  (**23**), (1*R*)-*M*-(1*R*) and (1*R*)-*S*-(1*R*) [46]. Code for atoms as in Fig. 1, with darkest medium size balls representing F atoms. Hydrogen atoms not shown.

An important family of poly- $\beta$ -diketonate-based metallocycles are made of ligands exhibiting two acetylacetonate moieties linked through the central carbon atom, either directly (in the case of  $H_2L_1$ ), or by a spacer. The reported spacers are of three types (see Table 1); 1,3-benzenediylbis(methylene) ( $H_2L_8$ ), 2,7-naphthalenediylbis(methylene) ( $H_2L_9$ ) or 1,3':1'',1'''-terphenyl-4,4''-bis(methylene) ( $H_2L_{10}$ ). The only cyclic cluster prepared with the ligand  $H_2L_1$  is a rare chiral square with formula  $[Co_4(L_1)_4(bpya)_4]$  (**24**, Fig. 4) [36], structurally related to complex **8** (see above), where each  $Co^{II}$  is now bound to one bipyridylamine ligand (instead of two), and constitutes one  $90^\circ$

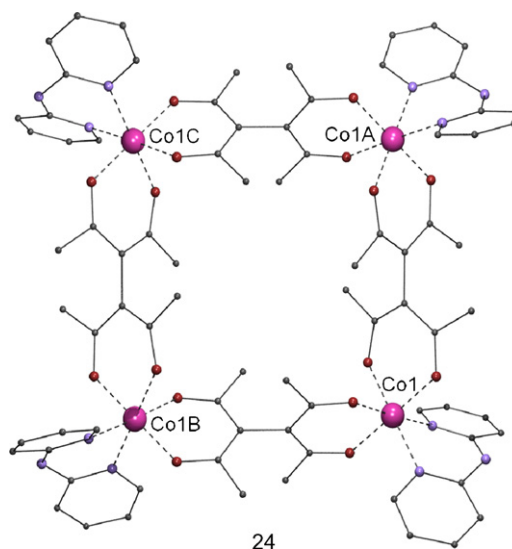
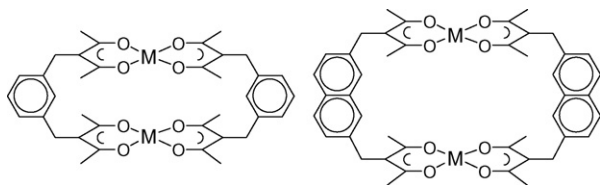


Fig. 4. PovRay representation of metallocycle  $[Co_4(L_1)_4(bpya)_4]$  (**24**) [36]. Code for atoms as in Fig. 1. Hydrogen atoms not shown.



Scheme 6. Representation of metallocycles made with ligands H<sub>2</sub>L8 (left) and H<sub>2</sub>L9 (right).

corner of the square through coordination to two L1<sup>2−</sup> ligands. In the analogous manner to complex **8**, the metal ions within the square display ferromagnetic interactions as a result of the mutual orientation of their magnetic orbitals.

Co-facial dinuclear complexes displaying metallacyclophanes with H<sub>2</sub>L8 and H<sub>2</sub>L9 (Scheme 6) have become a classical motif in coordination chemistry. The first complex of the *m*-phenylene ligand characterized by X-ray diffraction is [Cu<sub>2</sub>(L8)<sub>2</sub>] (**25**) [47], whereas the first 2,7-naphthalenediyl congener is [Cu<sub>2</sub>(L9)<sub>2</sub>] (**26**) [48], the structures of which are both represented in Scheme 6. It is clear that both structures possess an internal cavity that could be occupied by guest molecules. This was achieved for complex **26**, the cavity of which is large enough to host a variety of N-based bidentate ligands by simultaneous coordination to both metals. Some of these ligands are pyrazine (pz) and derivatives of this molecule, piperazine (ppz) or 1,4-diazabicyclo[2.2.2]octane (dabco). The X-ray structure of the resulting host–guest system has been obtained for the complexes [Cu<sub>2</sub>(L9)<sub>2</sub>(2-Mepz)] (**27**, 2-Mepz = 2-methylpyrazine) [49], [Cu<sub>2</sub>(L9)<sub>2</sub>(2,5-Me<sub>2</sub>pz)] (**28**, 2,5-Me<sub>2</sub>pz = 2,5-dimethylpyrazine) [35] and [Cu<sub>2</sub>(L9)<sub>2</sub>(dabco)] (**29**, Fig. 5) [48]. The reactivity of the ligand H<sub>2</sub>L8 with low-valent vanadium sources is very interesting. It was expected to form co-facial complexes analogous to complex **25** (see Scheme 6, left). Instead, reactions in THF with [VX<sub>3</sub>(thf)<sub>3</sub>] (V<sup>III</sup>; X = Cl, Br) and [VCl<sub>2</sub>(tmeda)<sub>2</sub>] (V<sup>II</sup>; tmeda = tetramethylethylenediamine) lead to complexes [V<sub>2</sub>X<sub>2</sub>(L8)<sub>2</sub>] (V<sup>III</sup>; X = Cl (**30**), Br (**31**); Fig. 6, top) and [V<sub>2</sub>(tmeda)<sub>2</sub>(L8)<sub>2</sub>] (V<sup>II</sup>; **32**; Fig. 6, bottom), respectively [50]. Interestingly, it was observed that the conformation in these complexes was different from the sought co-facial arrangement, perhaps as a result of the tendency of the V<sup>III</sup> and V<sup>II</sup> ions to coor-

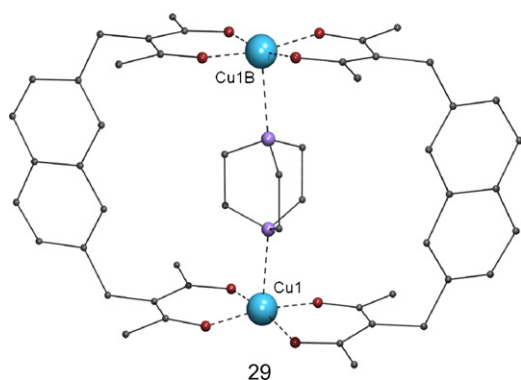


Fig. 5. PovRay representation of host–guest metallocycle [Cu<sub>2</sub>(L9)<sub>2</sub>(dabco)] (**29**) [48]. Code for atoms as in Fig. 1. Hydrogen atoms not shown.

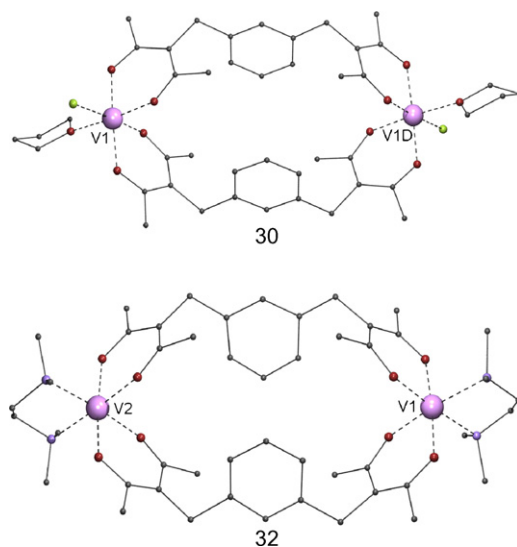


Fig. 6. PovRay representation of metallocycles [V<sub>2</sub>Cl<sub>2</sub>(L8)<sub>2</sub>] (**30**, top) and [V<sub>2</sub>(tmeda)<sub>2</sub>(L8)<sub>2</sub>] (**32**; bottom) [50]. Code for atoms as in Fig. 1, with lightest medium size balls representing Cl atoms. Hydrogen atoms not shown.

dinate in octahedral geometries. Compounds **30**, **31** and **32** are among the very few acetylacetonate-based low-valent vanadium complexes ever reported.

In a very interesting expansion of the above work, the ligand containing two acac units separated by a terphenyl–bismethylene moiety (H<sub>2</sub>L10) was prepared and concluding experimental evidence for the formation of the corresponding metallomacrocyclic [Cu<sub>2</sub>(L10)<sub>2</sub>] (**33**) was produced [51]. The capacity of this receptor to host larger molecules than observed for complex **26** was demonstrated with the synthesis and characterization of its 4,4′-bipyridine adduct [Cu<sub>2</sub>(L10)<sub>2</sub>(4,4′-bpy)] (**34**, Fig. 7), showing that the macrocycle has the appropriate size and topology to bind this guest molecule by coordination of both of its N-donor sites.

The other category of poly-β-diketone ligands helping to form metallocycles have two 1,3-diketone groups linked by one of their external α-carbon atoms through a spacer. In almost all cases the spacer is a phenylene ring and depending on whether the diketone groups are attached to the ring in mutual *meta* or

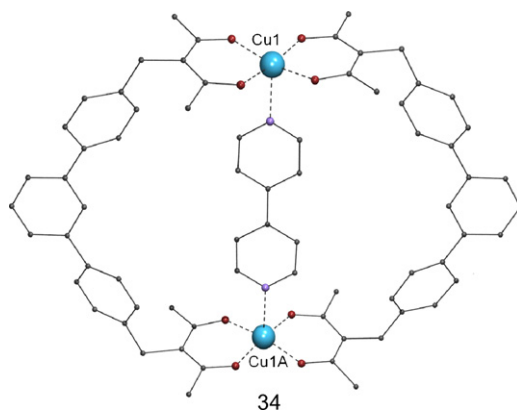
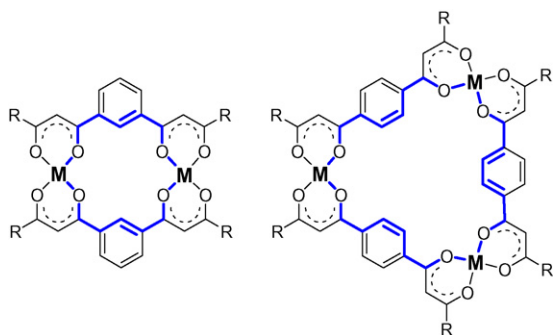


Fig. 7. PovRay representation of host–guest metallocycle [Cu<sub>2</sub>(L10)<sub>2</sub>(4,4′-bpy)] (**34**) [51]. Code for atoms as in Fig. 1. Hydrogen atoms not shown.



Scheme 7. Representation of dinuclear or trinuclear metallocycles made, respectively, with *m*-phenylene (left) or *p*-phenylene (right) spaced bis-β-diketonate ligands.

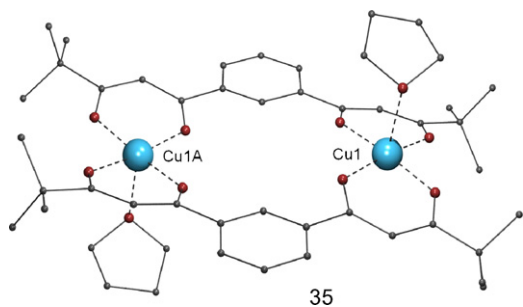


Fig. 8. PovRay representation of dinuclear metallocycle [Cu<sub>2</sub>(L14)<sub>2</sub>(thf)<sub>2</sub>] (35) [52]. Code for atoms as in Fig. 1. Hydrogen atoms not shown.

*para* positions, the ensuing macrocycles will be dinuclear or trinuclear (Scheme 7). Dinuclear metallocycles are obtained from reactions involving ligands of the type in the left side of Scheme 7 (H<sub>2</sub>L11 to H<sub>2</sub>L15) and CuCl<sub>2</sub> in the presence of a weak base (NaHCO<sub>3</sub>) [52]. In the absence of a co-ligand, these reactions are usually carried out in a coordinating solvent, such as pyridine or THF, in order to saturate the axial positions on the metal. A complex of this family, [Cu<sub>2</sub>(L14)<sub>2</sub>(thf)<sub>2</sub>] (35) is represented in Fig. 8. This class of metallocycles can be organized into more complicated superstructures if certain polydentate co-ligands are added to the reaction. These can be discrete, such as the dimer of

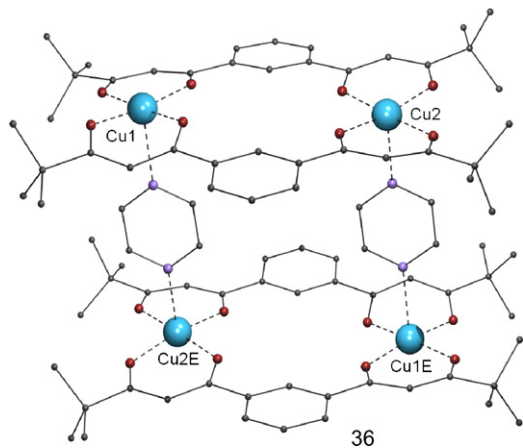


Fig. 9. PovRay representation of the dimer of dinuclear metallocycles [Cu<sub>2</sub>(L14)<sub>2</sub>(pz)<sub>2</sub>] (36) [52]. Code for atoms as in Fig. 1. Hydrogen atoms not shown.

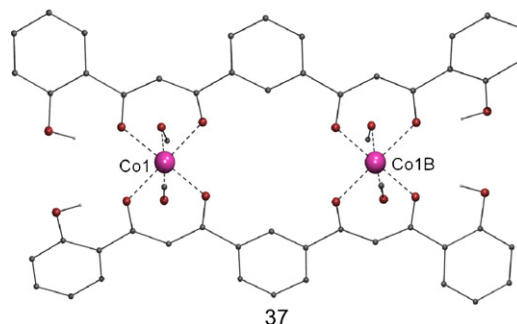


Fig. 10. PovRay representation of dinuclear metallocycle [Co<sub>2</sub>(H<sub>2</sub>L17)<sub>2</sub>(MeOH)<sub>2</sub>] (37) [53]. Code for atoms as in Fig. 1. Only H atoms from phenol groups shown.

metallocycles [Cu<sub>2</sub>(L14)<sub>2</sub>(pz)<sub>2</sub>] (36; Fig. 9), or arranged in infinite arrays (see Section 8). A collection of ligands related to the bis-β-diketone H<sub>2</sub>L15 has been prepared that have OH groups attached to the aromatic rings disposed near the 1,3-dicarbonyl moieties, so as to facilitate the assembly of arrays of closely spaced metals (ligands H<sub>3</sub>L16, H<sub>4</sub>L17, H<sub>4</sub>L18 and H<sub>5</sub>L19, Table 1). However, if the reaction conditions are not sufficiently basic to deprotonate the phenolic protons; in fact these ligands act in the same manner as does H<sub>2</sub>L15 and the formation of dinuclear metallocycles with coordinated solvents is also observed, such as [Co<sub>2</sub>(H<sub>2</sub>L17)<sub>2</sub>(MeOH)<sub>2</sub>] (37; Fig. 10). Thus, a large group of dinuclear complexes of these phenol-derived ligands have been obtained with Cu<sup>II</sup> [53–55], Co<sup>II</sup> [53,56,57], Mn<sup>II</sup> [53,58,59] and Ni<sup>II</sup> [53,56,59]. The presence of the OH groups in these ligands may play a role in the configuration of certain complexes; for example, the analogue [Mn<sub>2</sub>(H<sub>2</sub>L16)<sub>2</sub>(py)<sub>4</sub>] (38; Fig. 11) displays a very unusual conformation, probably caused by a combination of internal hydrogen bonds involving the OH groups. The possible magnetic-exchange interaction between the metals within this collection of dinuclear complexes was found to be negligible.

A smaller poly-β-diketonate based dinuclear macrocycle (12-member macrocycle) is the complex [Co<sub>2</sub>(L20)<sub>2</sub>(py)<sub>4</sub>] (39; Fig. 12) [60]. This complex results from the (ligand based) aerial oxidation of the related complex [Co<sub>2</sub>(L21)<sub>2</sub>(py)<sub>4</sub>] (40), the 3D structure of which is not available. The oxidation of the 1,3,5,7-tetraketonate L21<sup>2-</sup> occurs at the carbonylcarbon

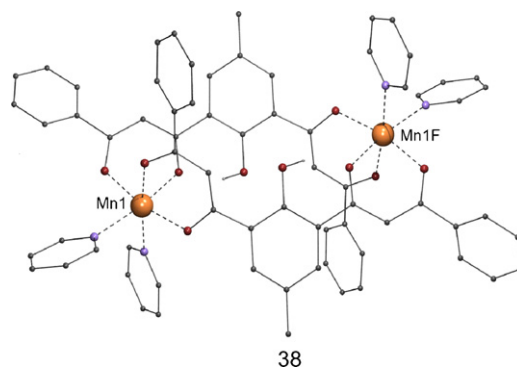


Fig. 11. PovRay representation of complex [Mn<sub>2</sub>(H<sub>2</sub>L16)<sub>2</sub>(py)<sub>4</sub>] (38) [58]. Code for atoms as in Fig. 1. Only H atoms from phenol groups shown.



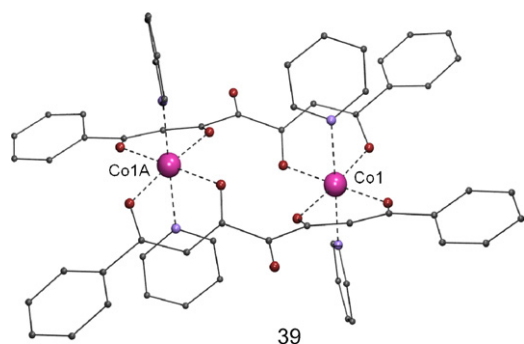


Fig. 12. PovRay representation of dinuclear metallocycle  $[\text{Co}_2(\text{L20})_2(\text{py})_4]$  (**39**) [60]. Code for atoms as in Fig. 1. Hydrogen atoms not shown.

located between positions 3 and 5. If the coordination pocket within these positions is occupied by a third metal (see Section 6), the oxidation does not take place.

Ligands featuring two 1,3-diketones linked sideways by a *p*-phenylene ( $\text{H}_2\text{L22}$ ,  $\text{H}_2\text{L23}$ ,  $\text{H}_2\text{L24}$ ,  $\text{H}_2\text{L25}$ ,  $\text{H}_2\text{L26}$ ) are suited to form trinuclear metallomacrocycles (see Scheme 7, right) through coordination to the equatorial plane of metals. Thus, a series of compounds of this kind have been prepared and characterized;  $[\text{Co}_3(\text{L26})_3(\text{py})_6]$  (**41**; Fig. 13),  $[\text{Ni}_3(\text{L26})_3(\text{py})_6]$  (**42**) – using the  $\text{Co}^{\text{II}}$  and  $\text{Ni}^{\text{II}}$  acetates as a metal source and proton acceptor – [61],  $[\text{Cu}_3(\text{L22})_3(\text{dmf})]$  (**43**) and  $[\text{Cu}_3(\text{L24})_3(\text{dmf})]$  (**44**) – where the metal source was  $\text{CuCl}_2$ , while  $\text{Na}_2\text{CO}_3$  was used as a base – [62]. The variable occupancy by guest molecules of the channels exhibited by complexes **41** and **42**, with preservation of the framework structure confers them the characteristics of “organic zeolites”.

The coordination of bidentate ligands to the axial positions of the metals in these macrocycles has been exploited to organize them into extended arrays (Section 8). Smaller trinuclear macrocycles are obtained with a related type of ligands, featuring two fused  $\beta$ -diketones (1,3,4,6-tetraketones,  $\text{H}_2\text{L27}$  and  $\text{H}_2\text{L28}$ ) allowing the formation of triangles, such as these within the sandwich complex  $[\text{NH}_4\text{OH}(\text{Cu}_3(\text{L28})_3)_2]$  (**45**, Fig. 14)

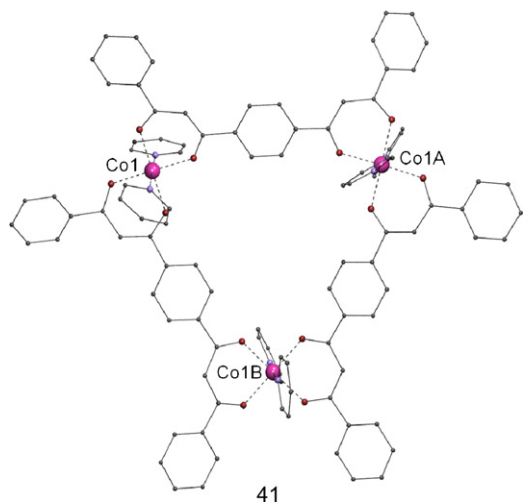


Fig. 13. PovRay representation of trinuclear metallocycle  $[\text{Co}_3(\text{L26})_3(\text{py})_6]$  (**41**) [61]. Code for atoms as in Fig. 1. Hydrogen atoms not shown.

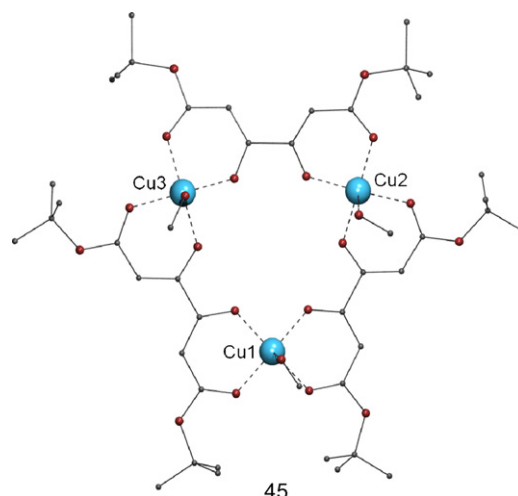
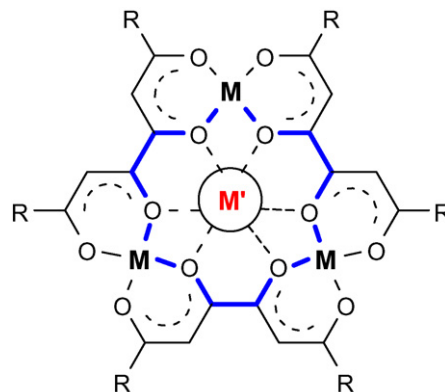


Fig. 14. PovRay representation of one of the trinuclear metallocycle units forming the sandwich complex  $[\text{NH}_4\text{OH}(\text{Cu}_3(\text{L28})_3)_2]$  (**45**) [63]. Hydrogen atoms not shown.



Scheme 8. Scheme of a metallacoronate formed by inclusion of a metal within a trinuclear metallocycle.

[63]. Many of these macrocycles have been characterized while featuring a central metal cation in the inner cavity, held by interactions with its oxygen donors (see Scheme 8). These systems have been perceived as the coordination chemistry analogues of coronates, therefore, the term “metallacoronate” has been coined to designate them [64]. One example is the crown complex  $[\text{Cu}_3\text{Ca}(\text{L27})_3(\text{NO}_3)_2(\text{H}_2\text{O})(\text{thf})]$  (**46**) [64], which exhibits an encapsulated  $\text{Ca}^{\text{II}}$  ion. Moreover, metallacoronates may be found organized as superior structures such as the double-deckers  $[\text{Cu}_3\text{Na}(\text{L28})_3(\text{CuCl}_2)_2]$  (**47**) [64] and  $[\text{Cu}_3\text{Na}(\text{L27})_3(\text{BF}_4)(\text{H}_2\text{O})(\text{thf})_2]$  (**48**), or the triple-decker  $[(\text{Cu}_3\text{Na}(\text{L27})_3)_3(\text{BF}_4)_2(\text{thf})_2](\text{BF}_4)$  (**49**) [65]. In the presence of cations that are too large to fit into the central cavity, metallacrowns may form ether sandwich complexes, as is the case with  $\text{K}^{\text{I}}$  in  $\text{K}[\text{Cu}_3(\text{L28})_3(\text{MeOH})_3]_2(\text{MeO})$  (**50**) [64].

## 5. Metallohelicates

Metallohelicates have become one of the archetypal categories of metallasupramolecular architectures [66]. Most examples are made with N-based polynucleating ligands, nev-

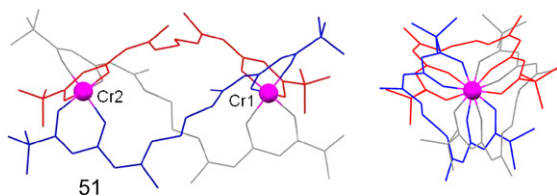


Fig. 15. Mercury representation of dinuclear metallohelicate  $[\text{Cr}_2(\text{L29})_3]$  (**51**) as viewed from the side (left) and along the molecular axis (right) [67]. Metals represented as balls and rest of the atoms as sticks. Hydrogen atoms not shown.

ertheless, a few interesting examples can be found involving only bis- $\beta$ -diketones in the coordination. Most of them are neutral, dinuclear triple-stranded helicates that share the formula  $[\text{M}_2\text{L}_3]$ , where  $\text{L}^{2-}$  is a doubly deprotonated bis- $\beta$ -diketonate and M is a trivalent metal. Because of their helical character, they possess absolute chirality, however, always racemic mixtures have been obtained. Interestingly, the first example,  $[\text{Cr}_2(\text{L29})_3]$  (**51**, Fig. 15) [67] was reported before the word *helicate* was coined to designate this now vast category of coordination complexes [68]. The ligand  $\text{H}_2\text{L29}$  was prepared by condensation of the triketone  $\text{H}_2\text{L41}$  (see below and Table 1) with ethylenediamine. The large flexibility of the strands in this helicate allows for the pronounced twisting along the axis observed in complex **51** (see Fig. 15, right). Considerably more rigid are the *m*-phenylene bis- $\beta$ -diketonate ligands  $\text{H}_2\text{L14}$ ,  $\text{H}_2\text{L30}$ ,  $\text{H}_2\text{L15}$  and  $\text{H}_2\text{L31}$ . Reaction of these ligands with various sources of  $\text{M}^{\text{III}}$  ions led to formation and crystallization of the family  $[\text{M}_2(\text{L15})_3]$  ( $\text{M}^{\text{III}} = \text{Ti}^{\text{III}}$ , **52**;  $\text{V}^{\text{III}}$ , **53**;  $\text{Mn}^{\text{III}}$ , **54**;  $\text{Fe}^{\text{III}}$ , **55**; see Fig. 16) [69,70],  $[\text{Fe}_2(\text{L30})_3]$  (**56**) [71] and  $[\text{Fe}_2(\text{L14})_3]$  (**57**) [52], which has been recently expanded to the group of lanthanides  $[\text{Ln}_2(\text{L15})_3]$  ( $\text{Ln}^{\text{III}} = \text{Eu}^{\text{III}}$ , **58**;  $\text{Nd}^{\text{III}}$ , **59**;  $\text{Sm}^{\text{III}}$ , **60**;  $\text{Y}^{\text{III}}$ , **61**;  $\text{Gd}^{\text{III}}$ , **62**), also including  $[\text{Ln}_2(\text{L31})_3]$  ( $\text{Ln}^{\text{III}} = \text{Eu}^{\text{III}}$ , **63**;  $\text{Nd}^{\text{III}}$ , **64**) [72]. This family clearly contains the most complete homologous series of metallohelicates available. As can be observed in Fig. 16 (right) this type of ligand permits a much lower degree of twisting. Another remarkable example in this category of helicates is the compound  $[\text{Fe}_2(\text{L32H})_3][\text{FeCl}_4]_3$  (**65**; Fig. 17) [73], obtained from the reaction of  $\text{FeCl}_3$  with the ligand  $\text{H}_2\text{L32}$ . The latter features a pyridin-2,6-diyl moiety separating the diketones instead of one *m*-phenylene spacer. Interestingly, during the course of this reaction, the proton from one of the 1,3-diketone groups of  $\text{H}_2\text{L32}$  is transferred to the

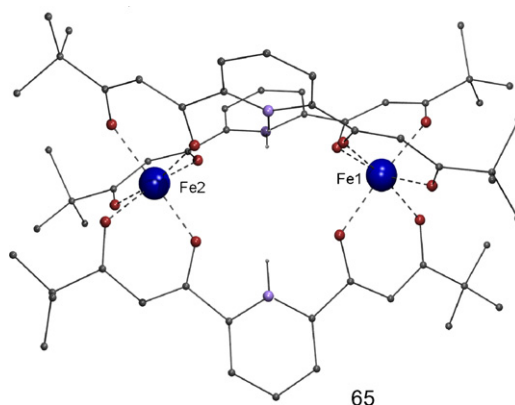


Fig. 17. PovRay representation of the cationic dinuclear metallohelicate of  $[\text{Fe}_2(\text{L32H})_3][\text{FeCl}_4]_3$  (**65**) [73]. Code for atoms as in Fig. 1. Only pyridinium H atoms shown.

pyridyl N-atom, while the second proton is not retained by the ligand. The final system thus compensates the extra three positive charges of the complex with stabilisation by three  $[\text{FeCl}_4]^-$  anions. This might have been a consequence of the absence of a suitable proton acceptor in this reaction, which otherwise would have conducted to formation of the hypothetical product “ $[\text{Fe}_2(\text{L32})_3]$ ”. Recent progress in this area has consisted in the preparation and study of enantiomerically pure helicates of this class by introducing absolute chirality into the ligand [74]. Thus, the chiral tetraketone  $\text{H}_2\text{L33}$  was prepared in the conventional manner (see Section 2) by using a chiral building block, which served to synthesize pure enantiomeric helicates  $[\text{Fe}_2(\text{L33})_3]$  (**66**; Fig. 18) and  $[\text{Ga}_2(\text{L33})_3]$  (**67**). Both compounds are soluble and stable in non-polar solvents. This allowed to follow the host–guest properties of **67** by  $^1\text{H}$  NMR, which was shown to encapsulate  $\text{Li}^+$  cations within its internal cavity, to form the metallacryptate  $[\text{Li} \subset \text{Ga}_2(\text{L33})_3](\text{ClO}_4)$  (**68**). More recently, this ligand has served for the preparation of a rare example of triple-stranded helicate of a divalent metal,  $\text{Ni}^{\text{II}}$ , in form of the complex  $(\text{pyH})_2[\text{Ni}_2(\text{L33})_3]$  (**69**) [75]. Finally, there are claims, as suggested by mass spectrometry and luminescence properties, that a quadruple-stranded helicate has been isolated and characterized;  $(\text{Hpip})_2[\text{Eu}_2(\text{L15})_4]$  (**70**; Hpip = piperidinium cation) [72].

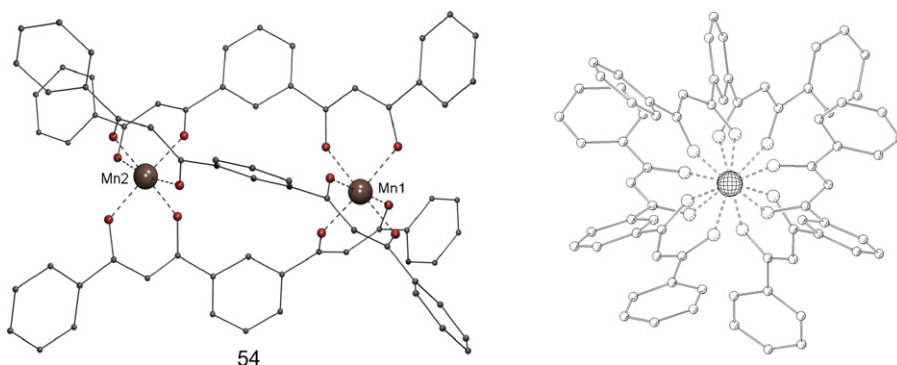


Fig. 16. Representation of dinuclear metallohelicate  $[\text{Mn}_2(\text{L15})_3]$  (**54**) [69] viewed from the side (left, PovRay; code for atoms as in Fig. 1) and along the molecular axis (right, Platon; large balls, metal; medium balls, oxygen; small balls, carbon; hydrogen atoms not shown).

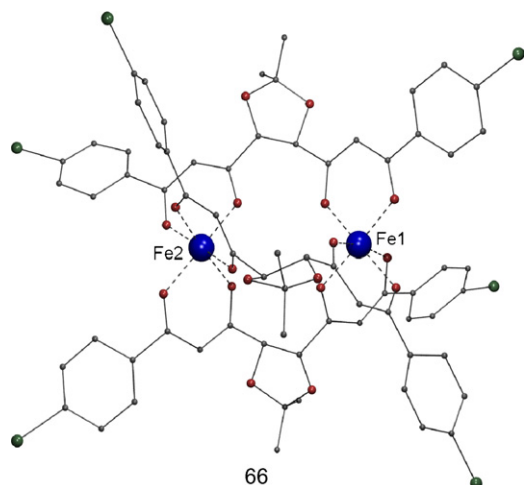
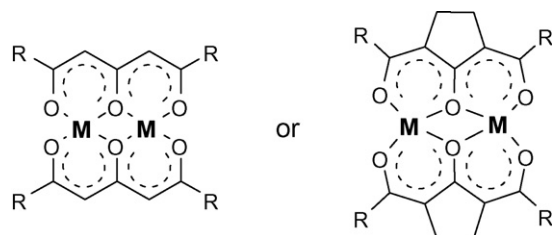


Fig. 18. Representation of the chiral dinuclear metallohelicate  $[\text{Fe}_2(\text{L}33)_3]$  (**66**) [74]. Code for atoms as in Fig. 1, with second largest balls representing Br.

## 6. Linear arrays

Ligands displaying side-wise connected 1,3-diketone groups oriented “parallel” to each other may form linear arrays of metals upon coordination. Two types have been already categorized; (i) dinuclear complexes assembled by two ligands with two  $\beta$ -diketones separated by *m*-phenylene have been grouped as metallomacrocycles (Section 3), (ii) dinuclear assemblies featuring three ligands twisted helically along the molecular axis have been considered as helicates (Section 5). Many complexes other than these from the above two groups can be called linear arrays. Ligands with two fused diketones (such as the 1,3,5-triketones  $\text{H}_2\text{L}34$  to  $\text{H}_2\text{L}42$ ) form dinuclear complexes with the metals bridged by the central oxygen atom that we classify as the smallest possible linear arrays. A large collection of homometallic dinuclear complexes exists with the basic structure shown in Scheme 9, where each metal  $\text{M}^{\text{II}}$  completes its coordination sphere with one or two axial monodentate ligands. The formulae of these compounds are  $[\text{Cu}_2(\text{L})_2(\text{S})_2]$  [76–79] or  $[\text{M}_2(\text{L})_2(\text{S})_4]$  ( $\text{M}^{\text{II}} = \text{Co}^{\text{II}}, \text{Ni}^{\text{II}}; \text{L}^{2-} = 1,3,5\text{-triketone}; \text{S} = \text{py}, \text{H}_2\text{O}, \text{or MeOH}$ ) [80–82]. One of the early motivations of this work was to gain insights into the mechanism of magnetic super-exchange, by studying a family of dinuclear compounds of different paramagnetic 3d metals sharing the same structural features and metal environment. In all cases the coupling was found to be antiferromagnetic. Later, investigations were focused on identifying the effect on the coupling caused by the



Scheme 9. Representation of the structure of dinuclear complexes formed with 1,3,5-triketones.

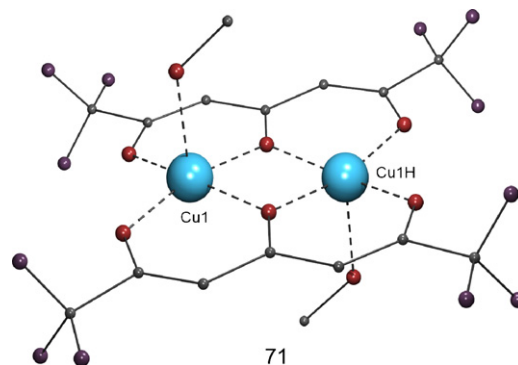


Fig. 19. PovRay representation of complex  $[\text{Cu}_2(\text{L}42)_2(\text{MeOH})_2]$  (**71**) [83]. Code for atoms as in Fig. 1, with darkest medium size balls representing F atoms. Hydrogen atoms not shown.

electronic properties of ligand substituents [83]. Thus, electron-withdrawing groups (such as  $-\text{CF}_3$  in  $[\text{Cu}_2(\text{L}42)_2(\text{MeOH})_2]$  (**71**) in Fig. 19) were found to cause a decrease of the super-exchange, presumably because they led to a decreased spin density on the bridging oxygen atoms.

In a step further with respect to the above family of dinuclear complexes, 1,3,5,7-tetraketone ligands such as  $\text{H}_3\text{L}21$  were expected to form the corresponding trinuclear complexes. This was only achieved in form of the heterometallic clusters with formula  $[(\text{UO}_2)_2\text{M}(\text{L}21)_2(\text{py})_4]$  ( $\text{M}^{\text{II}} = \text{Cu}^{\text{II}}$ , **72**;  $\text{Zn}^{\text{II}}$ , **73**;  $\text{Ni}^{\text{II}}$ , **74**;  $\text{Co}^{\text{II}}$ , **75**;  $\text{Mn}^{\text{II}}$ , **76**;  $\text{Fe}^{\text{II}}$ , **77**) [84,85]. In these complexes (see Fig. 20 for **74**),  $\text{UO}_2^{2+}$  groups are located at both ends of the polyketonates, adopting a pentagonal bipyramidal geometry and allowing the central pocket of the ligands to accommodate an  $\text{M}^{\text{II}}$  metal in an octahedral geometry. These are all prepared from the reaction of both salts,  $(\text{UO}_2)(\text{OAc})_2$  and  $\text{M}(\text{OAc})_2$ , ( $\text{OAc} = \text{acetate}$ ) with  $\text{H}_3\text{L}21$  in a  $\text{MeOH}/\text{py}$  solvent mixture. The reason why the homometallic trinuclear clusters are not obtained is likely the fact that the donors of the tetraketonates are not perfectly linear (see Fig. 20). Therefore, a trimetallic array is only observed if some of the metals can be accommodated with rather distorted coordination environments and large bond distances, as is the case with uranium within complexes **72** thru **77**.

An important class of trinuclear heterometallic linear clusters are formed with ligands that consist of two  $\beta$ -diketones separated by a pyridin-2,6-diyl moiety, such as  $\text{H}_2\text{L}32$ ,  $\text{H}_2\text{L}43$ ,

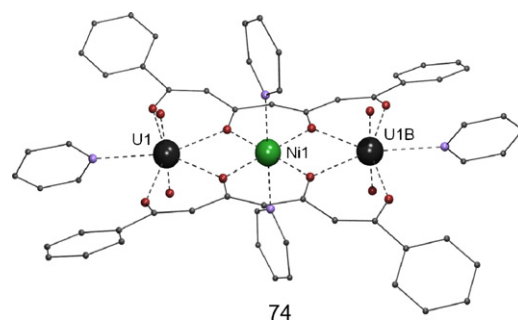
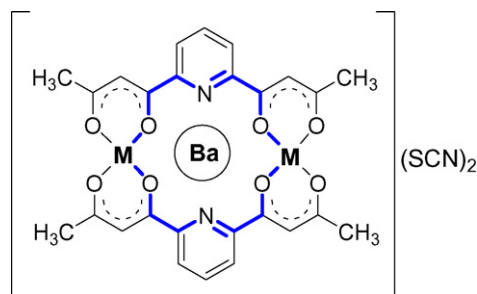


Fig. 20. PovRay representation of heterotrimeric complex  $[(\text{UO}_2)_2\text{Ni}(\text{L}21)_2(\text{py})_4]$  (**74**) [85]. Code for atoms as in Fig. 1, with darker largest balls representing U. Hydrogen atoms not shown.





Scheme 10. Representation of the structure of trinuclear heterometallic linear arrays obtained by inclusion and coordination of a metal within the inner cavity of dinuclear complexes of  $H_2L43$ .

$H_2L44$  and  $H_2L45$ . These ligands exhibit two types of coordination sites; the chelating 1,3-diketones and the pocket formed by the central pyridyl group together with one O-atom from each diketone. They are therefore, well suited for the assembly of heterometallic complexes. In this group of compounds, the external sites of the ligands are occupied by two  $3d M^{II}$  or  $M^{III}$  metal ions, and the central site may accommodate one alkali, one alkaline earth, or one lanthanide ion. Presumably, the earliest examples are two complexes with proposed formulae  $[M_2Ba(L43)_2](SCN)_2$  ( $M = Cu^{II}$ , **78a**;  $Ni^{II}$ , **78b**), the suggested structure of which is represented on Scheme 10 [86]. The latter scheme emphasizes the fact that this type of complexes can be viewed as “metallacoronates” in the same terms as defined above (see Section 4). The recent single-crystal structure of the nitrate derivatives of complexes **78a** and **78b**, namely  $[Cu_2Ba(L43)_2(NO_3)_2(MeOH)_2]$  (**79a**) and  $[Ni_2Ba(L43)_2(NO_3)_2(MeOH)_2(H_2O)_3]$  (**79b**) [87] reveal that the metals are not only coordinated by  $L43^{2-}$ , but also by counter-ions and solvent molecules. Together with the last two complexes, the corresponding derivatives with  $Pb^{II}$  instead of  $Ba^{II}$  were reported, i.e.  $[M_2Pb(L43)_2(NO_3)_2(MeOH)_2(H_2O)_2]$  ( $M = Cu^{II}$ , **80a**, Fig. 21;  $Ni^{II}$ , **80b**). The molecular structures show that the ion  $Pb^{II}$ , with an ionic radius of 1.32 Å, fits perfectly within the metallocrown, whereas the  $Ba^{II}$  ion (radius of 1.50 Å) is too large to reside in the cavity and is thus displaced 0.5–0.8 Å outside of it. If the  $3d$  metal is  $Co^{II}$ , the same kind of trinuclear units are obtained, which dimerize into more complex architectures with formulae  $[Co_2Pb(L43)_2(NO_3)(MeOH)_4]_2(NO_3)_2$  (**81**) and  $[Co_2Ba(L43)_2(NO_3)_2(MeOH)_2(H_2O)_2]_2$  (**82**), by virtue of  $NO_3^-$  bridges. With regard to lanthanides, a remarkable synthetic effort led to the crystal structure of a family of 15 linear complexes with the formula  $[Cu_2Ln(L43)(NO_3)_3(S)_2]$  ( $S = MeOH, H_2O$  or  $DMF$ ;  $Ln = La^{III}$ , **83**, Fig. 22;  $Ce^{III}$ , **84**;  $Pr^{III}$ , **85**;  $Nd^{III}$ , **86**;  $Sm^{III}$ , **87**;  $Eu^{III}$ , **88**;  $Gd^{III}$ , **89**;  $Tb^{III}$ , **90**;  $Dy^{III}$ , **91**;  $Ho^{III}$ , **92**;  $Er^{III}$ , **93**;  $Tm^{III}$ , **94**;  $Yb^{III}$ , **95**;  $Lu^{III}$ , **96**;  $Y^{III}$ , **97**) [88,89]. This allowed a comprehensive investigation aimed at elucidating the nature of the magnetic super-exchange between  $Cu^{II}$  and lanthanide ions. This task is complicated by the fact that all trivalent lanthanides ( $Ln^{III}$ ) with the exception of  $La^{III}$ ,  $Lu^{III}$  and  $Y^{III}$  (diamagnetic) and  $Gd^{III}$ , have their spin and orbital angular momenta coupled, and this phenomenon masks the effect of the magnetic exchange. The

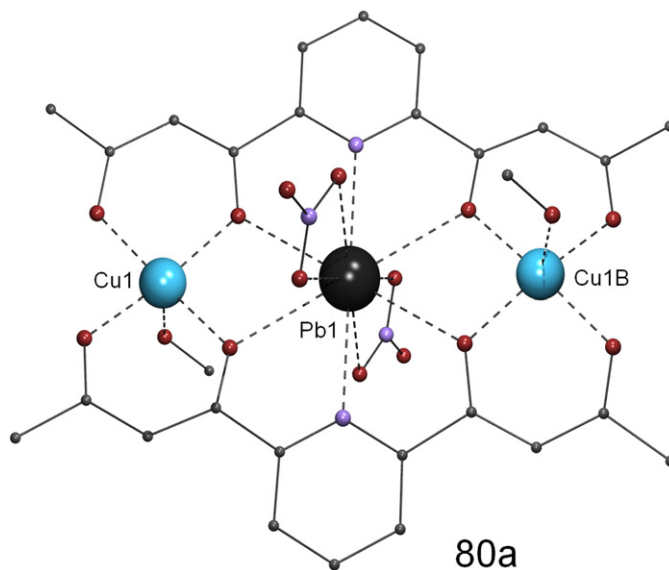


Fig. 21. PovRay representation of heterotrinnuclear complex  $[Cu_2Pb(L43)_2(NO_3)_2(MeOH)_2(H_2O)_2]$  (**80a**) [87]. Code for atoms as in Fig. 1, with darker largest balls representing Pb. Hydrogen atoms not shown.

study was conducted by comparing the magnetic properties of this group of compounds with these of the corresponding  $[Zn^{II}Ln^{III}Zn^{II}]$  analogues, whenever their preparation was possible. This allowed concluding that the coupling with  $Cu^{II}$  was antiferromagnetic for  $Ce^{III}$ ,  $Pr^{III}$ ,  $Nd^{III}$  and  $Sm^{III}$  and ferromagnetic for  $Tb^{III}$ ,  $Dy^{III}$ ,  $Ho^{III}$ ,  $Er^{III}$  and  $Gd^{III}$ . The linear complexes  $[Cu_2M(L46)(MeOH)_2](OAc)$  ( $M = K^I$ , **98**;  $Rb^I$ , **99**;  $Cs^I$ , **100**) [90] are related to this class of compounds. In this case, the spacer between the diketonates contains two ether functions, which are appropriate to establish interactions with alkali metals. The flexibility of the ligand  $L46^{2-}$  permits the inclusion of metals with disparate sizes as are  $K^I$ ,  $Rb^I$  and  $Cs^I$ .

Octahedral  $3d$  metal ions such as  $Fe^{III}$  tend to coordinate to three 1,3-diketone chelating units. Therefore, the

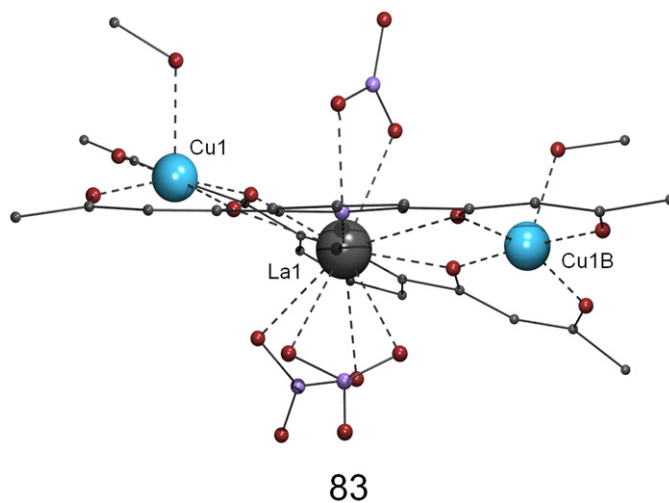


Fig. 22. PovRay representation of heterotrinnuclear complex  $[Cu_2La(L43)(NO_3)_3(MeOH)_2]$  (**83**) [89]. Code for atoms as in Fig. 1, with darker largest balls representing La. Hydrogen atoms not shown.

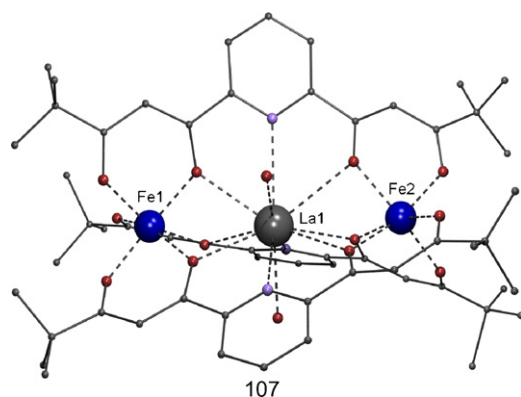


Fig. 23. PovRay representation of the heterotrinnuclear complex cation of  $[\text{Fe}_2\text{La}(\text{L32})_3(\text{H}_2\text{O})_2][\text{FeCl}_4]_3$  (**107**) [91]. Code for atoms as in Fig. 1, with darker largest balls representing La. Hydrogen atoms not shown.

pyridyl-spaced ligands  $\text{H}_2\text{L32}$ ,  $\text{H}_2\text{L43}$ ,  $\text{H}_2\text{L44}$ ,  $\text{H}_2\text{L45}$  will form complexes wrapped by three ligands that are related to the triple stranded helicates described above (Section 6). These will constitute linear heterometallic trinuclear clusters through incorporation of another metal in the central cavity, which can be of different categories, namely; (i) alkali metals, such as in  $[\text{Fe}_2\text{K}(\text{L32})_3](\text{PF}_6)$  (**101**) [71],  $[\text{Fe}_2\text{K}(\text{L44})_3](\text{PF}_6)$  (**102**) and  $[\text{Fe}_2\text{K}(\text{L45})_3][\text{FeCl}_4]$  (**103**) [91], (ii) alkaline-earth metals, e.g.  $[\text{Fe}_2\text{Sr}(\text{L32})_3(\text{H}_2\text{O})][\text{FeCl}_4]_2$  (**104**) [73],  $[\text{Fe}_2\text{Ba}(\text{L32})_3(\text{H}_2\text{O})][\text{FeCl}_4]_2$  (**105**) [91] and (iii) lanthanides, as in the case of  $[\text{Fe}_2\text{La}(\text{L43})_3(\text{thf})(\text{H}_2\text{O})][\text{FeCl}_4]_3$  (**106**) [73] or  $[\text{Fe}_2\text{La}(\text{L32})_3(\text{H}_2\text{O})_2][\text{FeCl}_4]_3$  (**107**, see Fig. 23) [91]. A clear analogy is observed between this collection of triple stranded coordination compounds encapsulating a central variable metal, and the classical cryptates. Therefore, these species have been called “metallacryptates” [71].

A homometallic linear cluster,  $[\text{Ni}_3(\text{py})_2(\text{OAc})_2(\text{L33})_2]$  (**108**, Fig. 24) [75], is formed with a bis- $\beta$ -diketonate ligand that does not feature a spacer with donor groups, but is flexible enough to allow the internal oxygens of the  $\beta$ -diketonates to bridge the central  $\text{Ni}^{\text{II}}$  ion to the external ones. In this complex, the presence

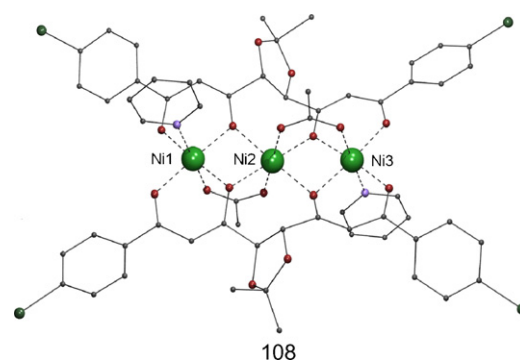


Fig. 24. PovRay representation of the trinuclear complex linear array  $[\text{Ni}_3(\text{py})_2(\text{OAc})_2(\text{L33})_2]$  (**108**) [75]. Code for atoms as in Fig. 1, with second largest balls representing Br. Hydrogen atoms not shown.

of  $\text{OAc}^-$  ions acting as additional bridges of the metals probably helps to the stabilisation of the linear array.

The *m*-phenoldiyl spaced bis- $\beta$ -diketonate ligand  $\text{H}_3\text{L16}$  may also coordinate to central ions to form linear arrays. Interestingly, if  $\text{H}_3\text{L16}$  is made to react with  $\text{M}(\text{OAc})_2$  ( $\text{M}^{\text{II}} = \text{Mn}^{\text{II}}$ ,  $\text{Co}^{\text{II}}$ ) in a coordinating solvent, the result are dinuclear complexes also containing solvent molecules as ligands (see Section 4), but in a non-donor solvent, triple-stranded trinuclear complexes,  $[\text{M}_3(\text{HL16})_3]$  ( $\text{M}^{\text{II}} = \text{Mn}^{\text{II}}$ , **109**, Fig. 25 (right), [92];  $\text{Co}^{\text{II}}$ , **110**; [57]) are obtained that do not need to incorporate any additional ligand for complete occupation of the metals' coordination sites. Interestingly, the trinuclear and the corresponding dinuclear complexes can be interconverted into each other by simply dissolving each solid into the appropriate solvent (Fig. 25) [58]. The ligand  $\text{HL16}^{2-}$  in complexes **109** and **110** retains the proton of the phenol group and this is the cause of the asymmetry of these linear arrays.

Another asymmetric trinuclear complex is  $[\text{Mn}_3(\text{HL19})_2(\text{py})_6]$  (**111**, Fig. 26) [56]. The asymmetry is not only related to the occupation of coordination pockets within the ligand, but also to the distribution of manganese oxidation states throughout the linear array; we find thus

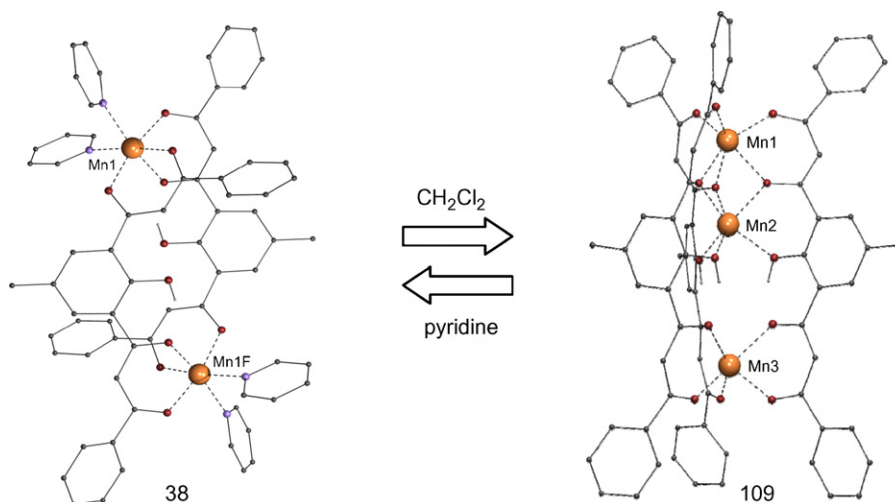


Fig. 25. PovRay representation of the asymmetric trinuclear linear array  $[\text{Mn}_3(\text{HL16})_3]$  (**109**, right) and the related dinuclear complex  $[\text{Mn}_2(\text{H}_2\text{L16})_2(\text{py})_4]$  (**38**, left), emphasizing the solvent-controlled interconversion between them [58]. Code for atoms as in Fig. 1. Only H atoms from phenol groups shown.

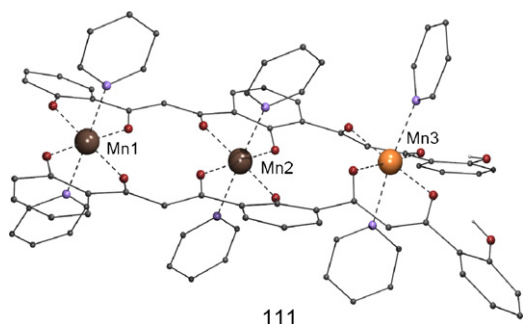


Fig. 26. PovRay representation of the asymmetric trinuclear linear array  $[\text{Mn}_3(\text{HL19})_2(\text{py})_6]$  (**111**) [56]. Code for atoms as in Fig. 1, where the  $[\text{Mn}^{\text{III}}\text{Mn}^{\text{III}}\text{Mn}^{\text{II}}]$  sequence is emphasized by making  $\text{Mn}^{\text{III}}$  darker than  $\text{Mn}^{\text{II}}$ . Only H atoms from phenol groups shown.

in complex **111** a unique  $[\text{Mn}^{\text{III}}\text{Mn}^{\text{III}}\text{Mn}^{\text{II}}]$  sequence. This compound was discovered accidentally from the oxidation and rearrangement of an all  $\text{Mn}^{\text{II}}$  complex, and could then be prepared directly from the comproportionation of  $\text{Mn}^{\text{II}}$  and  $\text{Mn}^{\text{VII}}$  in the molar ratio 6.5:1. It displays antiferromagnetic exchange interactions and a spin ground state of  $S = 5/2$ .

Ligand  $\text{H}_5\text{L19}$  displays seven oxygen donor atoms disposed linearly (see drawing included in Table 1) and therefore, holds the potential of assembling a large number of metal atoms. Its reaction with  $\text{Mn}(\text{OAc})_2$  in DMF yields the zig–zag tetranuclear linear array  $[\text{Mn}_4(\text{OAc})_2(\text{H}_2\text{L19})_2(\text{dmf})_4]$  (**112**, Fig. 27). In this complex, the central phenol group of  $\text{H}_2\text{L19}^{3-}$  is deprotonated and helps to the bridging of the metals, which is also assisted by  $\mu\text{-OAc}^-$  ligands in a similar manner to complex **108**. An almost identical complex,  $[\text{Mn}_4(\text{OAc})_2(\text{H}_2\text{L19})_2(\text{py})_5]$  (**113**), is obtained from pyridine [93].

A very interesting tetranuclear linear array is observed within complex  $[\text{Cu}_4(\text{L47})_2(\text{py})_4]$  (**114**, Fig. 28) [94], where the ligand  $\text{L48}^{4-}$  is a bis- $\beta$ -triketone that keeps the metals together as two separate dinuclear groups. This compound was sought in order to obtain molecular systems capable of undergoing multielectron transfer processes. Complex **114** exhibits two reversible reduction waves at very close potentials that correspond to the transfer of a total of four electrons. The dinuclear moieties within the molecule are very strongly coupled antiferromagnetically. A compound is known related to **114** that features  $\text{Fe}^{\text{III}}$  instead of

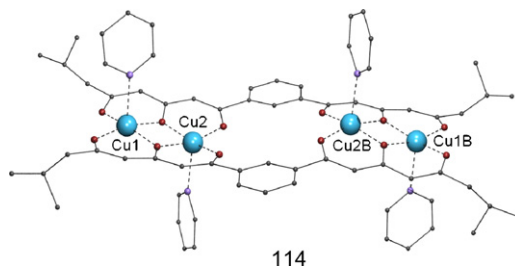


Fig. 28. PovRay representation of the tetranuclear cluster (pair of pairs)  $[\text{Cu}_4(\text{L47})_2(\text{py})_4]$  (**114**) [94]. Code for atoms as in Fig. 1. Hydrogen atoms not shown.

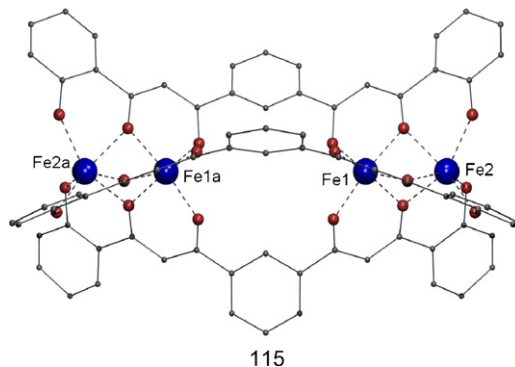


Fig. 29. PovRay representation of the tetranuclear cluster (pair of pairs)  $[\text{Fe}_4(\text{L17})_3]$  (**115**) [95]. Code for atoms as in Fig. 1. Hydrogen atoms not shown.

$\text{Cu}^{\text{II}}$ . Its formula is  $[\text{Fe}_4(\text{L17})_3]$  (**115**, Fig. 29), where  $\text{H}_4\text{L17}$  is a bis- $\beta$ -diketone with two phenol groups at both extremes. Three completely deprotonated ligands bridge and wrap the chain of four trivalent iron centers to saturate all their octahedral coordination sites and compensate 12 positive charges [95].

## 7. Polynuclear cage complexes

Many of the metal coordination clusters stabilized with poly- $\beta$ -diketone ligands do not fit any of the definitions used for the above groups of compounds and are gathered in this section. An interesting class is composed by tetranuclear compounds with open structures that are bridged exclusively by the diketone-like ligands, which maintain the metals well separated from each other at the vertices of regular tetrahedrons. Complexes  $(\text{NH}_4)[\text{Fe}_4(\text{L48})_6]$  (**116**, Fig. 30) and  $(\text{NH}_4)[\text{Fe}_4(\text{L49})_6]$  (**117**) [96] fall under this category. Ligands  $\text{H}_2\text{L48}$  and  $\text{H}_2\text{L49}$  are obtained *in situ* during cluster formation from oxalyl chloride and the corresponding dialkyl malonate in the presence of a strong base and  $\text{FeCl}_2$ . The final clusters are made by one  $\text{Fe}^{\text{II}}$  and three  $\text{Fe}^{\text{III}}$  ions that cannot be distinguished crystallographically (because of statistical disorder), but are clearly detected by Mössbauer spectroscopy. Both complexes encapsulate an  $\text{NH}_4^+$  cation that compensates one negative charge (See right part of Fig. 30). In a similar manner, the analogous complexes with  $\text{Mn}^{\text{II}}$ ,  $\text{Co}^{\text{II}}$  and  $\text{Ni}^{\text{II}}$  have been obtained [97], as described by the formulae  $(\text{NH}_4)_4[\text{Mn}_4(\text{L48})_6]$  (**118**),  $(\text{NH}_4)_4[\text{Co}_4(\text{L48})_6]$  (**119**) and  $(\text{NH}_4)_4[\text{Ni}_4(\text{L48})_6]$  (**120**). In these complexes, a larger number of cations are necessary to compensate the cluster's neg-

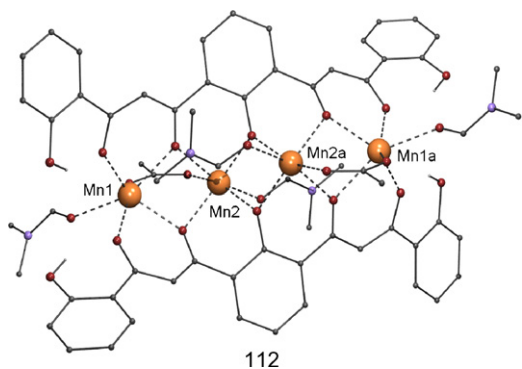


Fig. 27. PovRay representation of the tetranuclear linear cluster  $[\text{Mn}_4(\text{OAc})_2(\text{H}_2\text{L19})_2(\text{dmf})_4]$  (**112**) [56]. Code for atoms as in Fig. 1. Only H atoms from phenol groups shown.

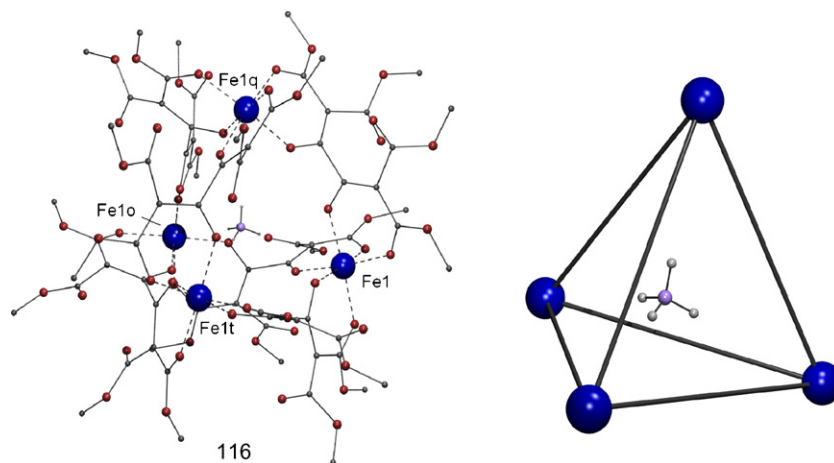


Fig. 30. PovRay representation of the tetrahedral cluster  $(\text{NH}_4)[\text{Fe}_4(\text{L48})_6]$  (**116**, left) [96]. The polyhedron formed by the metallic core, encapsulating an  $\text{NH}_4^+$  cation are emphasized (right). Code for atoms as in Fig. 1. Only H atoms from  $\text{NH}_4^+$  are shown.

ative charge and no ammonium was found encapsulated inside the cage. The *p*-phenylene spaced ligands  $\text{H}_2\text{L50}$  and  $\text{H}_2\text{L24}$  are very similar to  $\text{H}_2\text{L48}$  and  $\text{H}_2\text{L49}$ , now exhibiting a longer separation between the diketones. As a consequence, their reactions with  $\text{Fe}^{\text{III}}$  result in the formation of clusters related to **116** and **117**, with formulae  $[\text{Fe}_4(\text{L50})_6]$  (**121**) [98] and  $[\text{Fe}_4(\text{L24})_6]$  (**122**) (Fig. 31) [98] now exhibiting larger internal cavities. Complex **122** hosts a molecule of THF in this cavity that is observed through X-ray crystallography. Interestingly, the gallium counterpart of **122**, i.e.  $[\text{Ga}_4(\text{L24})_6]$  (**123**) [98], has been also prepared using an analogous procedure, and has been characterized by single crystal X-ray diffraction experiments.

Ligands  $\text{H}_2\text{L27}$  and  $\text{H}_2\text{L28}$ , which have the exact same coordination moiety as  $\text{H}_2\text{L48}$  and  $\text{H}_2\text{L49}$ , form octanuclear complexes  $[\text{M}_8\text{L}_8]$  ( $\text{M}^{\text{II}} = \text{Ca}^{\text{II}}, \text{Mn}^{\text{II}}, \text{Cd}^{\text{II}}, \text{L}^{2-} = \text{L27}^{2-}, \text{L28}^{2-}$ ) [65] instead of tetrahedral of the kind just described. Single crystals suitable for X-ray diffraction of the representative example  $[\text{Mn}_8(\text{L27})_8(\text{PrOH})_4]$  (**124**) could be obtained, which provided details of the molecular structure of this family of compounds (Fig. 32).

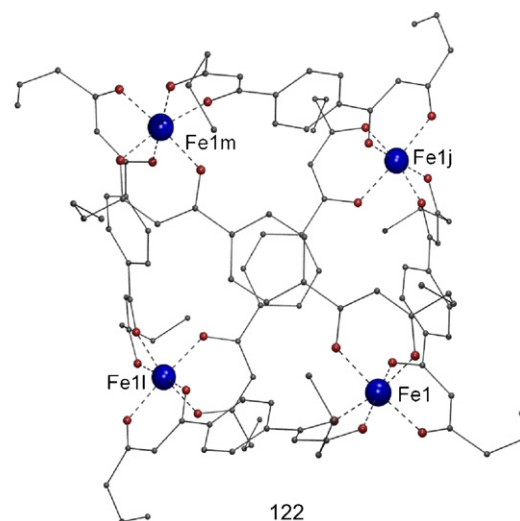


Fig. 31. PovRay representation of the tetrahedral cluster  $[\text{Fe}_4(\text{L24})_6]$  (**122**) [98]. Code for atoms as in Fig. 1. Hydrogen atoms not shown.

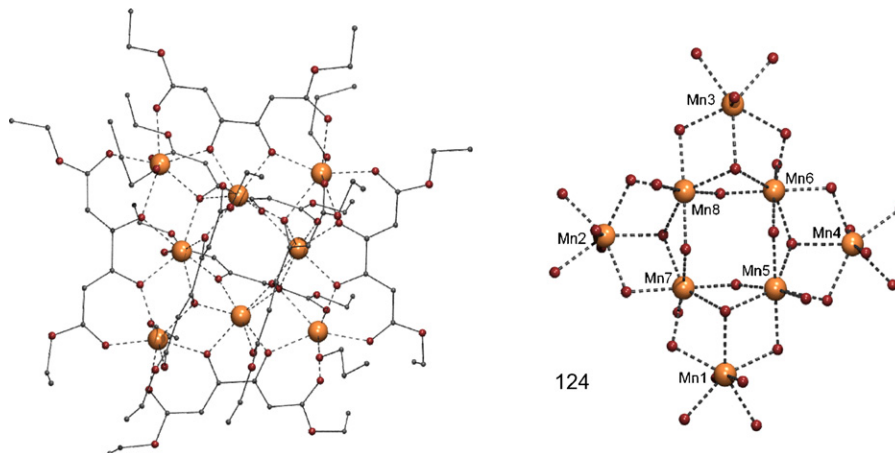


Fig. 32. PovRay representation of the octanuclear cluster  $[\text{Mn}_8(\text{L27})_8(\text{PrOH})_4]$  (**124**, left) [65]. The core is emphasized (right). Code for atoms as in Fig. 1. Hydrogen atoms not shown.



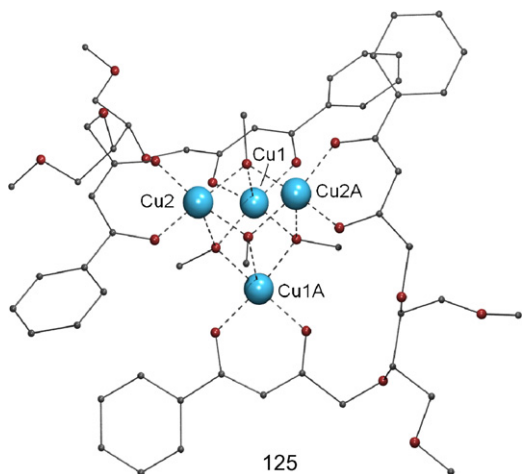
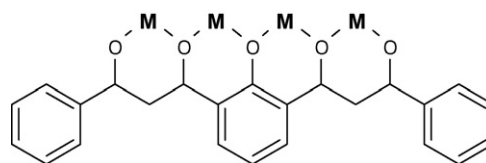


Fig. 33. PovRay representation of the chiral cubane-type cluster  $[\text{Cu}_4(\text{OMe})_4(\text{L51}^{(S,S)})_2]$  (**125**) [99]. Code for atoms as in Fig. 1. Hydrogen atoms not shown.

Formation of polynuclear clusters with poly- $\beta$ -diketones is favored in the presence of other smaller co-ligands that can act as additional bridges. The reaction in methanol of the enantiomerically pure ligand  $\text{H}_2\text{L51}^{(S,S)}$  with  $\text{Cu}(\text{OAc})_2$  in the 2:1 molar ratio affords the cubane cluster  $[\text{Cu}_4(\text{OMe})_4(\text{L51}^{(S,S)})_2]$  (**125**, Fig. 33) as a pure enantiomer, which features  $\mu_3$ -MeO-ligands [99]. The other enantiomer of this compound,



Scheme 11. Tetranuclear linear arrays formed by full occupancy of the coordination pockets available in  $\text{H}_3\text{L16}$ .

$[\text{Cu}_2(\text{OMe})_4(\text{L51}^{(R,R)})_2]$  (**126**), is prepared in the same manner by using  $\text{H}_2\text{L51}^{(R,R)}$  in the reaction. In the case of the nonanuclear cluster  $[\text{Ga}_9(\text{OH})_{10}(\text{L52})_8](\text{NO}_3)$  (**127**, Fig. 34) [100], where  $\text{H}_2\text{L52}$  is also a chiral ligand, the adventitious presence of water during its formation provides hydroxide ligands essential for the assembly of the polynuclear motif. Likewise, the octanuclear, analogous compounds  $[\text{Mn}_8\text{O}_2(\text{L53})_6]$  (**128**, Fig. 35) [101] and  $[\text{Co}_8\text{O}_2(\text{L32})_6]$  (**129**) [91], make use of  $\mu_3$ -oxide groups to cement the metal aggregate within a stable molecular species.

The bis- $\beta$ -diketone separated by an *m*-phenoldiyl group  $\text{H}_3\text{L16}$  was designed to assemble chains of four closely spaced metals (Scheme 11) within molecules. This was achieved for the case of  $\text{Cu}^{\text{II}}$  within the complex  $[\text{Cu}_8(\text{OMe})_8(\text{L16})_2(\text{ClO}_4)_2(\text{MeOH})_4]$  (**130**, Fig. 36) [54], which features the mentioned linear moiety in form of dimers bridged by  $\mu$ - and  $\mu_3$ -OMe<sup>−</sup> ligands.

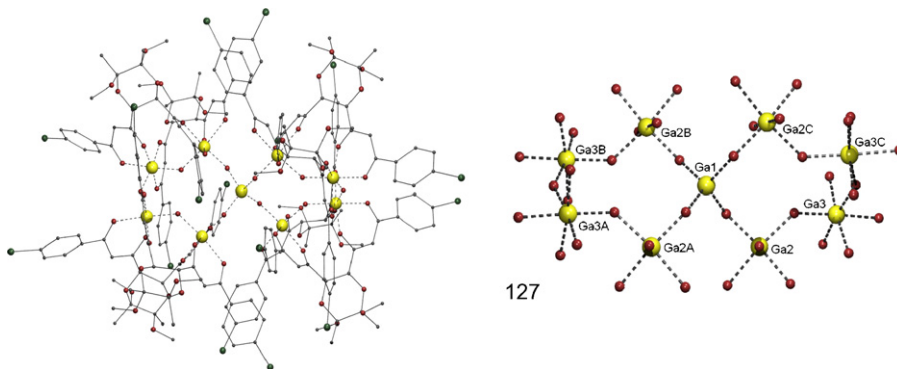


Fig. 34. PovRay representation of the nonanuclear cluster  $[\text{Ga}_9(\text{OH})_{10}(\text{L52})_8](\text{NO}_3)$  (**127**, left [100]; code for atoms as in Fig. 1, with second largest balls representing Br atoms; hydrogen atoms not shown). The core is emphasized (right; code for atoms as in Fig. 1).

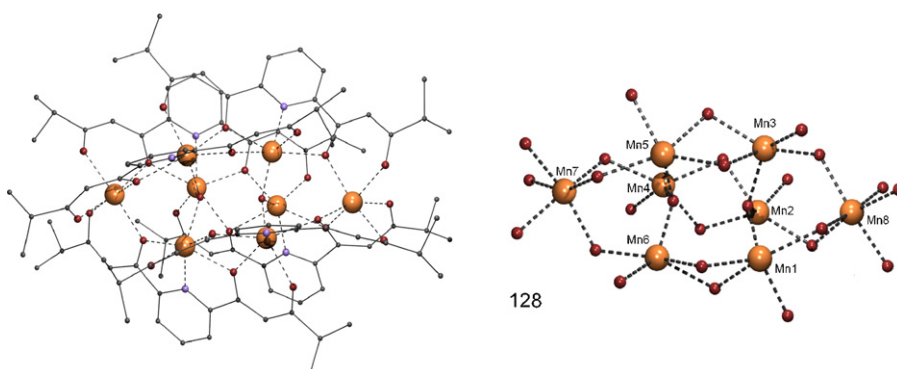


Fig. 35. PovRay representation of the octanuclear cluster  $[\text{Mn}_8\text{O}_2(\text{L53})_6]$  (**128**, left) [101]. The core is emphasized (right). Code for atoms as in Fig. 1. Hydrogen atoms not shown.

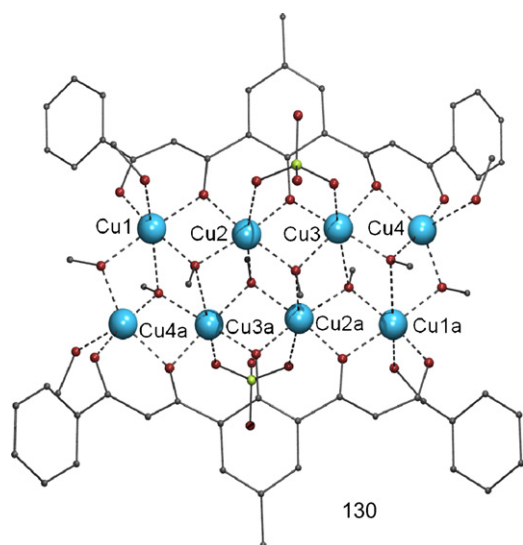


Fig. 36. PovRay representation of the octanuclear cluster  $[\text{Cu}_8(\text{OMe})_8(\text{L16})_2(\text{ClO}_4)_2(\text{MeOH})_4]$  (**130**) [54]. Code for atoms as in Fig. 1, with lightest medium size balls representing Cl. Hydrogen atoms not shown.

In a last category of cluster complexes, poly- $\beta$ -diketonate ligands help to bridge different polynuclear fragments together that would otherwise exist as stable independent species. Interesting examples are the supramolecular aggregates  $[\text{Mn}_4\text{O}_2(\text{RCO}_2)_6(\text{pz})(\text{H}_2\text{L18})]_2$  ( $\text{R} = \text{Me}$ , **131**, Fig. 37;  $\text{Ph}$ , **132**;  $p\text{-MePh}$ , **133**) and  $[\text{Fe}_4\text{O}_2(\text{PhCO}_2)_6(\text{pz})(\text{H}_2\text{L18})]_2$  (**134**), which consist of molecules containing two  $[\text{M}^{\text{III}}_4]$  fragments with a “butterfly” arrangement, very common in cluster coordination chemistry, brought together by the action of  $\text{H}_2\text{L18}^{2-}$ . The latter bis- $\beta$ -diketonate allows the  $[\text{M}^{\text{III}}_4]$  units to remain as *quasi* independent recognizable units while permitting these to weakly interact magnetically within the same molecule [102]. Another molecule exhibiting the same profile is the pair of oxido-centered and carboxylate bridged  $\text{Fe}^{\text{III}}$  triangles linked together again by  $\text{H}_2\text{L18}^{2-}$  ligands,  $[\text{Fe}_6\text{O}_2(\text{BzO})_{10}(\text{H}_2\text{L18})_2(\text{H}_2\text{O})_2]$  (**135**, Fig. 38) [102].

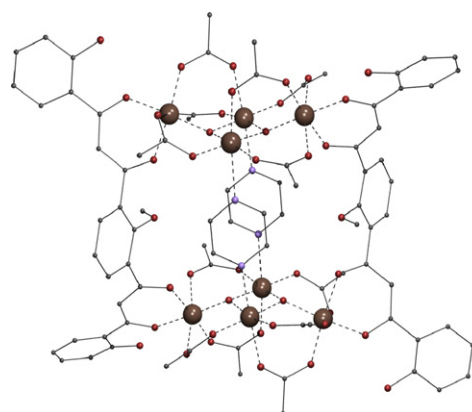


Fig. 37. PovRay representation of the octanuclear cluster  $[\text{Mn}_4\text{O}_2(\text{MeCO}_2)_6(\text{pz})(\text{H}_2\text{L18})]_2$  (**131**) [102]. The core is emphasized (right). Code for atoms as in Fig. 1. Hydrogen atoms not shown.

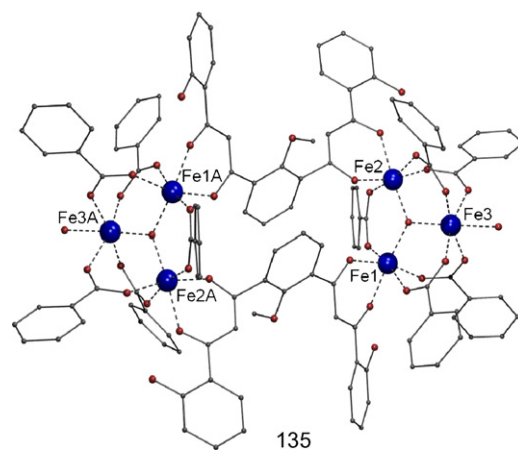
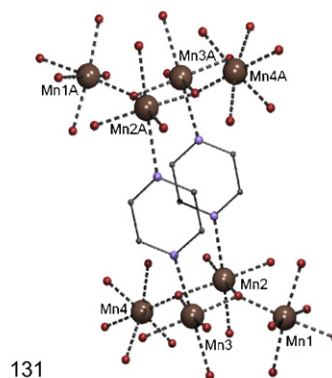


Fig. 38. PovRay representation of the hexanuclear cluster  $[\text{Fe}_6\text{O}_2(\text{BzO})_{10}(\text{H}_2\text{L18})_2(\text{H}_2\text{O})_2]$  (**135**) [102]. Code for atoms as in Fig. 1. Hydrogen atoms not shown.

## 8. Coordination polymers

Infinite arrays or polymers, clearly constitute the minority of the structurally characterized coordination species involving poly- $\beta$ -diketonates. The most likely reason is the difficulty in obtaining this type of compounds as single crystals, given the very scarce solubility that they usually exhibit. Nevertheless, a few very interesting examples exist, as detailed throughout the next few paragraphs. Interestingly, almost all coordination polymers described consist of the repetition of connected monomeric units that, themselves, fall within one of the categories proposed above to describe the discrete systems.

The compound  $[\text{Zn}(\text{L26})(\text{py})_2]_n \cdot n\text{py}$  (**136**, Fig. 39) [61] is one of the simplest polymers that can be obtained with poly- $\beta$ -diketonates. It consists of chains of octahedral  $\text{Zn}^{\text{II}}$  ions exhibiting pyridine axial ligands, solely connected through their equatorial positions by the  $p$ -phenylene spaced bis- $\beta$ -diketonate  $\text{L26}^{2-}$ . Interestingly, complexes with  $\text{Co}^{\text{II}}$  (**41**) and  $\text{Ni}^{\text{II}}$  (**42**) have exactly the same composition as (**136**), just by changing metals, but are organized as discrete trinuclear metallocycles (see Sec-



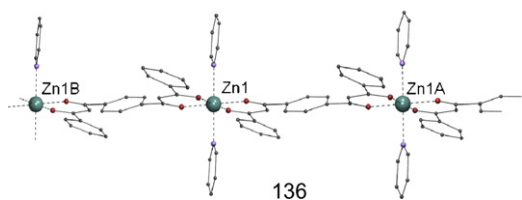


Fig. 39. PovRay representation of the coordination polymer  $[\text{Zn}(\text{L26})(\text{py})_2]_n \cdot n\text{py}$  (**136**) [61]. Code for atoms as in Fig. 1. Hydrogen atoms not shown.

tion 4 and Fig. 13). The conformation of the ligand (or “rotamer”, as termed by some authors) is the local structural feature that decides which of the two drastically different organizations is adopted, as illustrated in Scheme 12.

A more complicated polymer is the compound  $[\text{Cu}_2(\text{L1})(\text{bpya})_2(4,4'\text{-bpy})]_n(\text{O}_2\text{CCF}_3)_{2n}$  (**137**, Fig. 40) [40] composed by the succession of dinuclear entities containing the spacer  $(\text{L1})^{2-}$  (see Section 3), bridged to each other

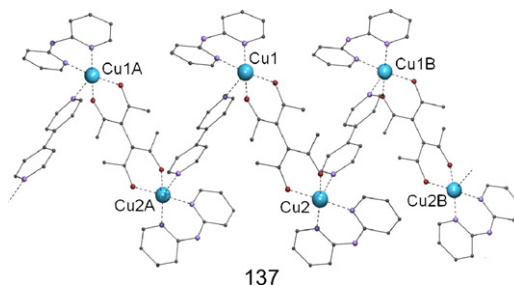
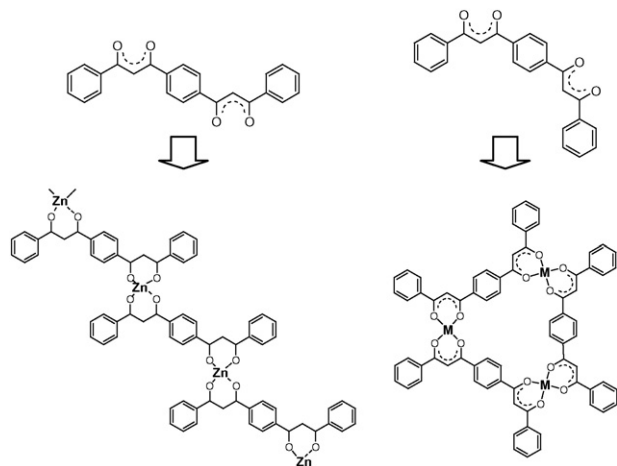


Fig. 40. PovRay representation of the polymer of dinuclear complexes  $[\text{Cu}_2(\text{L1})(\text{bpya})_2(4,4'\text{-bpy})]_n(\text{O}_2\text{CCF}_3)_{2n}$  (**137**) [40]. Code for atoms as in Fig. 1. Hydrogen atoms not shown.

by a bipyridyl ligand. Dinuclear or trinuclear metalocycles have also been found as part of polymeric arrays when linked by means of didentate N-donor ligands. Examples of the former are  $[\text{Cu}_2(\text{L14})_2(\text{azpy})]_n$  (**138**; azpy = 4,4'-*trans*-azopyridine) [52],  $[\text{Cu}_2(\text{L14})_2(\text{dps})]_n$  (**139**; dps = 4,4'-dipyridyl sulfide) and  $[\text{Cu}_2(\text{L14})_2(\text{xbp})]_n$  (**140**; xbp = 4,4'-(1,3-xylylene)-bis(3,5dimethylpyrazole)) [103], while some polymers of trinuclear metalocycles are known as  $[\text{Cu}_3(\text{L23})_3(\text{bpy})(\text{thf})]_n$  (**141**; bpy = 4,4'-bipyridine),  $[\text{Cu}_3(\text{L23})_3(\text{pz})(\text{thf})]_n$  (**142**; pz = pyrazine, Fig. 41, left) and  $[\text{Cu}_3(\text{L25})_3(\text{dabco})_3]_n$  (**143**; dabco = 1,4-diazabicyclo[2.2.2]-octane) [104]. Complexes **141** and **142** consist of chains with the trinuclear units linked to each other by only one ditopic ligand, whereas complex **143** exhibits a columnar structure where the bridges are triple (Fig. 41, right). The complex  $[\text{Cu}_3(\text{L24})_3(\text{hmt})]$  (**144**) [104], in turn, is a three-dimensional network built up from the linkage of trinuclear metalocycles by means of hexamethyltetramine, which disposes four tetrahedrally oriented nitrogen donor atoms for coordination to metals.

Another way of obtaining coordination polymers of well-defined poly- $\beta$ -diketonate assembled aggregates is through linkage by coordinating anions. This is the case for the infinite chains of octanuclear clusters  $[\text{Cu}_8(\text{OME})_8(\text{L16})_2(\text{NO}_3)_2]_n$  (**145**, Fig. 42) [105],  $[\text{Cu}_8(\text{OME})_8(\text{L16})_2\text{Cl}_2]_n$  (**146**) and  $[\text{Cu}_8(\text{OME})_{7.9}(\text{L16})_2\text{Br}_{2.1}]_n$  (**147**) [54]. In all three cases the



Scheme 12. Representation of the supramolecular organization into infinite chains (left) or discrete trinuclear metalohelicates (right) of complexes of  $\text{H}_2\text{L26}$  depending on the configuration adopted by the ligand.

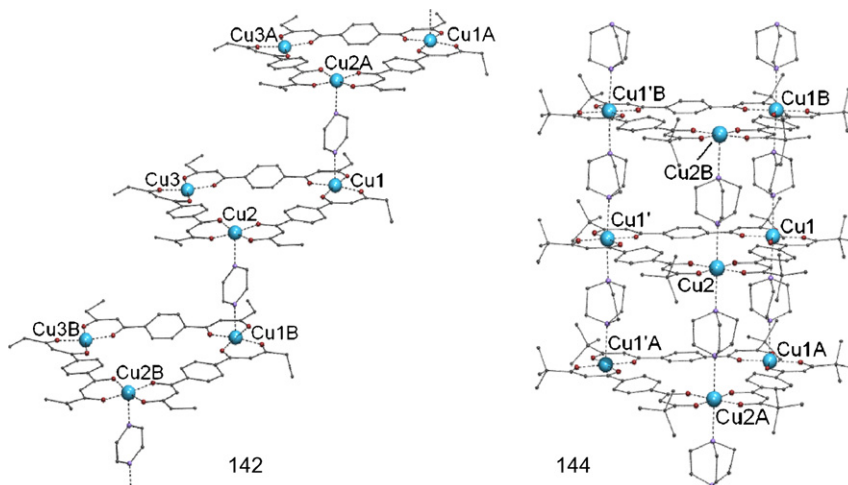


Fig. 41. PovRay representation of the ‘ladder-like’ cluster polymer  $[\text{Cu}_3(\text{L23})_3(\text{pz})(\text{thf})]_n$  (**142**, left) [104] and the columnar stack of trinuclear metalocycles  $[\text{Cu}_3(\text{L24})_3(\text{hmt})]$  (**144**) [104]. Code for atoms as in Fig. 1. Hydrogen atoms not shown.

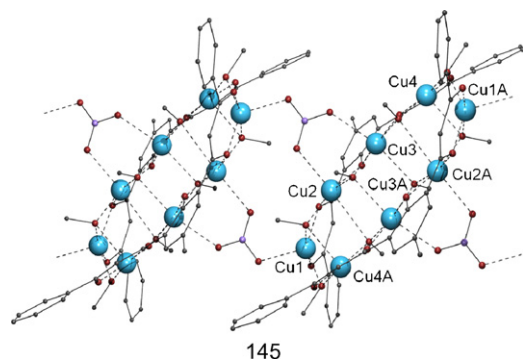


Fig. 42. PovRay representation of the polymer of octanuclear clusters  $[\text{Cu}_8(\text{OMe})_8(\text{L16})_2(\text{NO}_3)_2]_n$  (**145**) [105]. Code for atoms as in Fig. 1. Hydrogen atoms not shown.

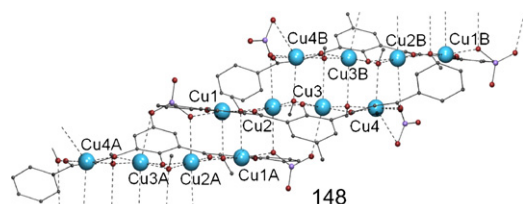


Fig. 43. PovRay representation of the infinite ladder of tetranuclear chains  $[\text{Cu}_4(\text{OMe})_3(\text{L16})(\text{NO}_3)_2(\text{H}_2\text{O})_{0.4}]_n$  (**148**) [54]. Code for atoms as in Fig. 1. Hydrogen atoms not shown.

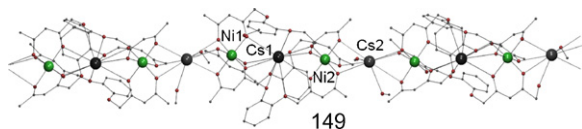


Fig. 44. PovRay representation of the infinite succession of  $\text{Cs}^{\text{I}}$  linked heterotrinnuclear clusters  $[\text{Cs}(\text{CsNi}_2(\text{L54})_3)]_n$  (**149**) [90]. Code for atoms as in Fig. 1, with darker largest balls representing Cs. Hydrogen atoms not shown.

repeating metallic unit is essentially the same, changing only the counter-ion, as provided by the  $\text{Cu}^{\text{II}}$  salt used for the reaction. The magnetic properties of these systems are dominated by the strong antiferromagnetic interactions within the octanuclear moieties. Slight changes in the stoichiometry lead to a related system,  $[\text{Cu}_4(\text{OMe})_3(\text{L16})(\text{NO}_3)_2(\text{H}_2\text{O})_{0.4}]_n$  (**148**, Fig. 43) [54], now formed by infinite ladders of bis- $\beta$ -diketonate templated  $[\text{Cu}_4]$  chains, bound more intimately to each other by  $\text{MeO}^-$  bridging ligands.

Finally, polymerization can occur between clusters that, themselves, provide donor sites to metal ions (through the so called “complex-as-ligand” approach), which in turn, permit to link the aggregates to each other. This is the case of the  $\text{Cs}^{\text{I}}$  linked chain of heterotrinnuclear clusters  $[\text{Cs}(\text{CsNi}_2(\text{L54})_3)]_n$  (**149**, Fig. 44), where the external oxygens of the 1,3-diketonates in  $\text{L54}^{2-}$  are the Lewis bases that facilitate the interaction with the  $\text{Cs}^{\text{I}}$  bridges [90].

## 9. Conclusions

The realization of this review has demonstrated that the class of poly- $\beta$ -diketone ligands is suited for the construction of supramolecular architectures, discrete and polymeric, with a

large variety of structures. The versatility in synthetic procedures allows for combination of 1,3-diketone moieties in a variety of topological arrangements, with the consequent geometrical richness of the resulting coordination assemblies. Synthetic flexibility has also permitted the incorporation of other functional or coordinating groups to these ligands, granting them the multi-component character. From the relatively scarce number of research groups currently engaged in the design, preparation and study of the coordination chemistry of poly- $\beta$ -diketonates, it is clear that the sub-discipline has not yet been fully explored and, therefore, holds great potential of development. One of the future challenges is that of obtaining molecule-based systems capable of fulfilling functions with technological applications. In this overview, the interest of some of the reviewed compounds for their optical or their magnetic properties has been hinted. Presumably, while this class of compounds gains more prominence, the potential in areas of technological interest will unfold. We hope that this review will constitute a useful reference and starting point in this direction.

## Acknowledgements

GA thanks the Spanish Ministry of Science and Education for a “Ramón y Cajal” Fellowship. The coordination of our research activities by the FP6 Network of Excellence “Magmanet” (contract number 515767) is also kindly acknowledged.

## References

- [1] S.L. James, *Chem. Soc. Rev.* 32 (2003) 276.
- [2] J.M. Lehn, *Angew. Chem. Int. Ed.* 295 (2002) 2400.
- [3] G.F. Swiegers, T.J. Malefetse, *Coord. Chem. Rev.* 225 (2002) 91.
- [4] E.C. Constable, P. Harverson, C.E. Housecroft, E. Nordlander, J. Olsson, *Polyhedron* 25 (2006) 437.
- [5] M. Fujita, *Struct. Bond.* 96 (2000) 177.
- [6] M. Albrecht, *Chem. Soc. Rev.* 27 (1998) 281.
- [7] E. Ingó, E. Zangrando, E. Alessio, *Eur. J. Inorg. Chem.* (2003) 2371.
- [8] J.L. Atwood, L.J. Barbour, M.J. Hardie, C.L. Raston, *Coord. Chem. Rev.* 222 (2001) 3.
- [9] D.J. Bray, J.K. Clegg, L.F. Lindoy, D. Schilter, *Adv. Inorg. Chem.* 59 (2007) 1.
- [10] L. Claisen, E.F. Ehrhardt, *Chem. Ber.* 22 (1889) 1009.
- [11] H. Meerwein, *Chem. Ber.* 66 (1933) 411.
- [12] Y.Y. Lim, W. Chen, L.L. Tan, X.Z. You, T.M. Yao, *Polyhedron* 13 (1994) 2861.
- [13] M.R. Maurya, *Coord. Chem. Rev.* 237 (2003) 163.
- [14] A.M. Trzeciak, B. Borak, Z. Ciunik, J.J. Ziolkowski, M.F.C.G. da Silva, A.J.L. Pombeiro, *Eur. J. Inorg. Chem.* (2004) 1411.
- [15] M. Doring, G. Hahn, M. Stoll, A.C. Wolski, *Organometallics* 16 (1997) 1879.
- [16] H. Hagen, J. Boersma, G. van Koten, *Chem. Soc. Rev.* 31 (2002) 357.
- [17] S.G. Bott, B.D. Fahlman, M.L. Pierson, A.R. Barron, *J. Chem. Soc., Dalton Trans.* (2001) 2148.
- [18] R.C. Smith, T.Z. Ma, N. Hoilien, L.Y. Tsung, M.J. Bevan, L. Colombo, J. Roberts, S.A. Campbell, W.L. Gladfelter, *Adv. Mater. Opt. Electron.* 10 (2000) 105.
- [19] T.J. Anderson, M.A. Neuman, G.A. Melson, *Inorg. Chem.* 12 (1973) 927.
- [20] H. Siegel, W. Eggers, Gerhartz (Eds.), *Ullmann's Encyclopaedia of Industrial Chemistry*, vol. A15, VCH Verlag, Weinheim, 1988, p. 77.
- [21] A.H. Lowrey, C. George, P. Dantonio, J. Karle, *J. Am. Chem. Soc.* 93 (1971) 6399.



- [22] J. Stary, The Solvent Extraction of Metal Chelates, Pergamon, Oxford, 1964, p. 51.
- [23] J.D. Woolins, Inorganic Experiments, VCH, Weinheim, Germany, 1994, p. 117.
- [24] S. Geremia, N. Demitri, J. Chem. Educ. 82 (2005) 460.
- [25] S. Shibata, S. Onuma, H. Inoue, Inorg. Chem. 24 (1985) 1723.
- [26] F.A. Cotton, R.C. Elder, Inorg. Chem. 4 (1965) 1145.
- [27] F.A. Cotton, R. Eiss, J. Am. Chem. Soc. 90 (1968) 38.
- [28] R.Y. Wang, D.T. Song, S.M. Wang, Chem. Commun. (2002) 368.
- [29] G. Aromí, S. Parsons, W. Wernsdorfer, E.K. Brechin, E.J.L. McInnes, Chem. Commun. (2005) 5038.
- [30] B.L. Chen, F.R. Fronczek, A.W. Maverick, Chem. Commun. (2003) 2166.
- [31] Y. Cui, H.L. Ngo, W.B. Lin, Chem. Commun. (2003) 1388.
- [32] S.R. Halper, M.R. Malachowski, H.M. Delaney, S.M. Cohen, Inorg. Chem. 43 (2004) 1242.
- [33] B.L. Chen, F.R. Fronczek, A.W. Maverick, Inorg. Chem. 43 (2004) 8209.
- [34] V.D. Vreshch, A.N. Chernega, J.A.K. Howard, J. Sieler, K.V. Domasevitch, Dalton Trans. (2003) 1707.
- [35] A.W. Maverick, M.L. Ivie, J.H. Waggenspack, F.R. Fronczek, Inorg. Chem. 29 (1990) 2403.
- [36] Y.S. Zhang, S.N. Wang, G.D. Enright, S.R. Breeze, J. Am. Chem. Soc. 120 (1998) 9398.
- [37] Y. Hoshino, S. Higuchi, J. Fiedler, C.Y. Su, A. Knodler, B. Schwederski, B. Sarkar, H. Hartmann, W. Kaim, Angew. Chem. Int. Ed. 42 (2003) 674.
- [38] Y. Fukuda, K. Mafune, Chem. Lett. (1988) 697.
- [39] J. Labuda, K. Mafune, Y. Fukuda, Bull. Chem. Soc. Jpn. 63 (1990) 2610.
- [40] Y.S. Zhang, S.R. Breeze, S.N. Wang, J.E. Greedan, N.P. Raju, L.J. Li, Can. J. Chem. 77 (1999) 1424.
- [41] X.P. Shen, J.Z. Zou, Z.G. Zha, Z. Xu, B.C. Yip, H.K. Fun, Chinese J. Inorg. Chem. 15 (1999) 641.
- [42] X.P. Shen, J.Z. Zou, Z.G. Zha, C.Y. Duan, Z. Xu, Chinese J. Inorg. Chem. 15 (1999) 793.
- [43] T. Koiwa, Y. Masuda, J. Shono, Y. Kawamoto, Y. Hoshino, T. Hashimoto, K. Natarajan, K. Shimizu, Inorg. Chem. 43 (2004) 6215.
- [44] O.E. Woisetschlager, A. Geisbauer, K. Polborn, W. Beck, Z. Anorg. All. Chem. 626 (2000) 766.
- [45] P. Scheer, V. Schurig, L. Walz, Synth. Met. 43 (1991) 4071.
- [46] V. Schurig, H. Gaus, P. Scheer, L. Walz, H.G. Vonschering, Angew. Chem. Int. Ed. 28 (1989) 1019.
- [47] A.W. Maverick, F.E. Klavetter, Inorg. Chem. 23 (1984) 4129–4130.
- [48] A.W. Maverick, S.C. Buckingham, Q. Yao, J.R. Bradbury, G.G. Stanley, J. Am. Chem. Soc. 108 (1986) 7430.
- [49] A.W. Maverick, D.R. Billodeaux, M.L. Ivie, F.R. Fronczek, E.F. Maverick, J. Inclusion Phenom. Macrocyclic Chem. 39 (2001) 19.
- [50] P.J. Bonitatebus, S.K. Mandal, W.H. Armstrong, Chem. Commun. (1998) 939.
- [51] G.J.E. Davidson, A.J. Baer, A.P. Cote, N.J. Taylor, G.S. Hanan, Y. Tanaka, M. Watanabe, Can. J. Chem. 80 (2002) 496.
- [52] J.K. Clegg, L.F. Lindoy, J.C. McMurtrie, D. Schilter, Dalton Trans. (2005) 857.
- [53] G. Aromí, C. Boldron, P. Gamez, O. Roubeau, H. Kooijman, A.L. Spek, H. Stoeckli-Evans, J. Ribas, J. Reedijk, Dalton Trans. (2004) 3586.
- [54] G. Aromí, J. Ribas, P. Gamez, O. Roubeau, H. Kooijman, A.L. Spek, S. Teat, E. MacLean, H. Stoeckli-Evans, J. Reedijk, Chem. -Eur. J. 10 (2004) 6476.
- [55] H. Kooijman, A.L. Spek, G. Aromí, P. Gamez, P.C. Berzal, W.L. Driessen, J. Reedijk, Acta Crystallogr. E 58 (2002) m223.
- [56] G. Aromí, P. Gamez, J. Krzystek, H. Kooijman, A.L. Spek, E.J. MacLean, S.J. Teat, H. Nowell, Inorg. Chem. 46 (2007) 2519.
- [57] G. Aromí, H. Stoeckli-Evans, S.J. Teat, J. Cano, J. Ribas, J. Mater. Chem. 16 (2006) 2635–2644.
- [58] G. Aromí, P. Gamez, O. Roubeau, P.C. Berzal, H. Kooijman, A.L. Spek, W.L. Driessen, J. Reedijk, Inorg. Chem. 41 (2002) 3673.
- [59] G. Aromí, P. Gamez, O. Roubeau, P. Carrero-Berzal, H. Kooijman, A.L. Spek, W.L. Driessen, J. Reedijk, Eur. J. Inorg. Chem. (2002) 1046.
- [60] R.L. Lintvedt, G. Ranger, C. Ceccarelli, Inorg. Chem. 24 (1985) 456.
- [61] D.V. Soldatov, A.S. Zanina, G.D. Enright, C.I. Ratcliffe, J.A. Ripmeester, Cryst. Growth Des. 3 (2003) 1005.
- [62] J.K. Clegg, L.F. Lindoy, B. Moubaraki, K.S. Murray, J.C. McMurtrie, Dalton Trans. (2004) 2417.
- [63] R.W. Saalfrank, N. Low, F. Hampel, H.D. Stachel, Angew. Chem. Int. Ed. 35 (1996) 2209–2210.
- [64] R.W. Saalfrank, N. Low, S. Kareth, V. Seitz, F. Hampel, D. Stalke, M. Teichert, Angew. Chem. Int. Ed. 37 (1998) 172–175.
- [65] R.W. Saalfrank, N. Low, B. Demleitner, D. Stalke, M. Teichert, Chem. Eur. J. 4 (1998) 1305–1311.
- [66] C. Piguet, G. Bernardinelli, G. Hopfgartner, Chem. Rev. 97 (1997) 2005.
- [67] R.L. Lintvedt, G. Ranger, C. Ceccarelli, Inorg. Chem. 24 (1985) 1819–1821.
- [68] J.M. Lehn, A. Rigault, J. Siegel, J. Harrowfield, B. Chevrier, D. Moras, Proc. Natl. Acad. Sci. U.S.A. 84 (1987) 2565.
- [69] V.A. Grillo, E.J. Seddon, C.M. Grant, G. Aromí, J.C. Bollinger, K. Folting, G. Christou, Chem. Commun. (1997) 1561.
- [70] M.M. Matsushita, T. Yasuda, R. Kawano, T. Kawai, T. Iyoda, Chem. Lett. (2000) 812.
- [71] R.W. Saalfrank, A. Dresel, V. Seitz, S. Trummer, F. Hampel, M. Teichert, D. Stalke, C. Stadler, J. Daub, V. Schunemann, A.X. Trautwein, Chem. -Eur. J. 3 (1997) 2058.
- [72] A.P. Bassett, S.W. Magennis, P.B. Glover, D.J. Lewis, N. Spencer, S. Parsons, R.M. Williams, L. De Cola, Z. Pikramenou, J. Am. Chem. Soc. 126 (2004) 9413.
- [73] R.W. Saalfrank, V. Seitz, D.L. Caulder, K.N. Raymond, M. Teichert, D. Stalke, Eur. J. Inorg. Chem. (1998) 1313.
- [74] M. Albrecht, S. Schmid, M. deGroot, P. Weis, R. Frohlich, Chem. Commun. (2003) 2526.
- [75] M. Albrecht, S. Dehn, G. Raahe, R. Frolich, Chem. Commun. (2005) 5690.
- [76] R.L. Lintvedt, M.D. Glick, B.K. Tomlonovic, D.P. Gavel, J.M. Kuszaj, Inorg. Chem. 15 (1976) 1633.
- [77] J. Overgaard, M.A. Chevallier, B.B. Iversen, Acta Crystallogr. E 61 (2005) M922.
- [78] M.J. Heeg, J.L. Mack, M.D. Glick, R.L. Lintvedt, Inorg. Chem. 20 (1981) 833.
- [79] A.B. Blake, L.R. Fraser, J. Chem. Soc., Dalton Trans. (1974) 2554.
- [80] P.D.W. Boyd, K.S. Lee, M. Zvagulis, Aust. J. Chem. 39 (1986) 1249.
- [81] J.M. Kuszaj, B. Tomlonov, D.P. Murtha, R.L. Lintvedt, M.D. Glick, Inorg. Chem. 12 (1973) 1297.
- [82] R.L. Lintvedt, L.L. Borer, D.P. Murtha, J.M. Kuszaj, M.D. Glick, Inorg. Chem. 13 (1974) 18.
- [83] J.W. Guthrie, R.L. Lintvedt, M.D. Glick, Inorg. Chem. 19 (1980) 2949.
- [84] R.L. Lintvedt, M.J. Heeg, N. Ahmad, M.D. Glick, Inorg. Chem. 21 (1982) 2350.
- [85] R.L. Lintvedt, B.A. Schoenfelner, C. Ceccarelli, M.D. Glick, Inorg. Chem. 23 (1984) 2867.
- [86] D.E. Fenton, J.R. Tate, U. Casellato, S. Tamburini, P.A. Vigato, M. Vidali, Inorg. Chim. Acta 83 (1984) 23.
- [87] T. Shiga, T. Nakanishi, M. Ohba, H. Okawa, Polyhedron 24 (2005) 2732.
- [88] T. Shiga, M. Ohba, H. Okawa, Inorg. Chem. 43 (2004) 4435.
- [89] T. Shiga, M. Ohba, H. Okawa, Inorg. Chem. Commun. 6 (2003) 15.
- [90] R.W. Saalfrank, H. Maid, N. Mooren, F. Hampel, Angew. Chem. Int. Ed. 41 (2002) 304.
- [91] R.W. Saalfrank, V. Seitz, F.W. Heinemann, C. Gobel, R. Herbst-Irmer, J. Chem. Soc., Dalton Trans. (2001) 599.
- [92] G. Aromí, P.C. Berzal, P. Gamez, O. Roubeau, H. Kooijman, A.L. Spek, W.L. Driessen, J. Reedijk, Angew. Chem. Int. Ed. 40 (2001) 3444.
- [93] G. Aromí, P. Gamez, C. Boldron, H. Kooijman, A.L. Spek, J. Reedijk, Eur. J. Inorg. Chem. (2006) 1940.
- [94] R.L. Lintvedt, J.K. Zehetmair, Inorg. Chem. 29 (1990) 2204.
- [95] G. Aromí, L.A. Barrios, et al., unpublished results.
- [96] R.W. Saalfrank, R. Burak, A. Breit, D. Stalke, R. Herbstirmer, J. Daub, M. Porsch, E. Bill, M. Muther, A.X. Trautwein, Angew. Chem. Int. Ed. 33 (1994) 1621.
- [97] R.W. Saalfrank, A. Stark, M. Bremer, H.U. Hummel, Angew. Chem. Int. Ed. Engl. 29 (1990) 311.
- [98] R.W. Saalfrank, B. Horner, D. Stalke, J. Salbeck, Angew. Chem. Int. Ed. 32 (1993) 1179.

- [99] R.W. Saalfrank, C. Schmidt, H. Maid, F. Hampel, W. Bauer, A. Scheurer, *Angew. Chem. Int. Ed.* 45 (2006) 315.
- [100] M. Albrecht, S. Dehn, R. Fröhlich, *Angew. Chem. Int. Ed.* 45 (2006) 2792.
- [101] R.W. Saalfrank, N. Low, S. Trummer, G.M. Sheldrick, M. Teichert, D. Stalke, *Eur. J. Inorg. Chem.* (1998) 559.
- [102] G. Aromí, E.C. Sañudo, et al., unpublished results.
- [103] J.K. Clegg, K. Gloe, M.J. Hayter, O. Kataeva, L.F. Lindoy, B. Moubaraki, J.C. McMurtrie, K.S. Murray, D. Schilter, *Dalton Trans.* (2006) 3977.
- [104] J.K. Clegg, L.F. Lindoy, J.C. McMurtrie, D. Schilter, *Dalton Trans.* (2006) 3114.
- [105] G. Aromí, P. Gamez, O. Roubeau, H. Kooijman, A.L. Spek, W.L. Driessen, J. Reedijk, *Angew. Chem. Int. Ed.* 41 (2002) 1168.
- [106] L.Y. Cho, J.R. Romero, *Tetrahedron Lett.* 36 (1995) 8757.
- [107] O.E. Woisetschlager, A. Geisbauer, K. Polborn, K. Sunkel, W. Beck, *Z. Anorg. Allg. Chem.* 625 (1999) 2164.
- [108] D.F. Martin, W.C. Fernelius, M. Shamma, *J. Am. Chem. Soc.* 81 (1959) 130.
- [109] A. Minami, R. Uchida, T. Eguchi, K. Kakinuma, *J. Am. Chem. Soc.* 127 (2005) 6148.
- [110] D.E. Fenton, C.M. Regan, U. Casellato, P.A. Vigato, M. Vidali, *Inorg. Chim. Acta* 44 (1980) L105.
- [111] D.F. Martin, M. Shamma, W.C. Fernelius, *J. Am. Chem. Soc.* 80 (1958) 4891.
- [112] G. Aromí, P. Gamez, P.C. Berzal, W.L. Driessen, J. Reedijk, *Synth. Commun.* 33 (2003) 11.
- [113] R.M. Sandifer, A.K. Bhattacharya, T.M. Harris, *J. Org. Chem.* 46 (1981) 2260.
- [114] M.L. Miles, T.M. Harris, C.R. Hauser, *J. Org. Chem.* 30 (1965) 1007.
- [115] T.P. Murray, T.M. Harris, *J. Am. Chem. Soc.* 94 (1972) 8253.
- [116] H.D. Stachel, M. Jungkenn, C. Kosergrnoss, H. Poschenrieder, J. Redlin, *Liebigs Ann. Chem.* (1994) 961.
- [117] J.F. Wishart, C. Ceccarelli, R.L. Lintvedt, J.M. Berg, D.P. Foley, T. Frey, J.E. Hahn, K.O. Hodgson, R. Weis, *Inorg. Chem.* 22 (1983) 1667.
- [118] A. El-Qisairi, P.M. Henry, *J. Organomet. Chem.* 603 (2000) 50.
- [119] R. Gleiter, G. Krennrich, M. Langer, *Angew. Chem. Int. Ed. Engl.* 25 (1986) 999.
- [120] X.Q. Han, R.A. Widenhoefer, *J. Org. Chem.* 69 (2004) 1738.
- [121] J.R. Bethell, P. Maitland, *J. Chem. Soc.* (1962) 3751.
- [122] D.L. Chizhov, K.I. Pashkevich, G.-V. Roeschenthaler, *J. Fluorine Chem.* 123 (2003) 267.
- [123] S. Ruhemann, *J. Chem. Soc.* (1912) 1729.
- [124] D.E. Fenton, S.E. Gayda, P. Holmes, *Inorg. Chim. Acta* 21 (1977) 187–189.
- [125] G.W. Buchanan, A. Moghimi, C.I. Ratcliffe, *Can. J. Chem.* 74 (1996) 1437.
- [126] J.T. Adams, C.R. Hauser, *J. Am. Chem. Soc.* 66 (1944) 1220.
- [127] P. Ruggli, A. Staub, *Helv. Chim. Acta* (1936) 962.
- [128] R.W. Saalfrank, B. Demleitner, H. Glaser, H. Maid, S. Reihls, W. Bauer, M. Maluenga, F. Hampel, M. Teichert, H. Krautscheid, *Eur. J. Inorg. Chem.* (2003) 822.
- [129] U. Berens, D. Leckel, S.C. Oepen, *J. Org. Chem.* 60 (1995) 8204.
- [130] Y. Kobuke, K. Kokubo, M. Munakata, *J. Am. Chem. Soc.* 117 (1995) 12751.